Active retreat of a Late Weichselian marine-terminating glacier: An example from Melasveit, W-Iceland

THORBJÖRG SIGFÚSDÓTTIR, ÍVAR ÖRN BENEDIKTSSON AND EMRYS PHILLIPS

Sigfúsdóttir, T., Benediktsson, Í. Ö. & Phillips, E.: Active retreat of a Late Weichselian marine-terminating glacier: An example from Melasveit, W-Iceland.

Large and complete glaciotectonic sequences formed by marine-terminating glaciers are rarely observed on land, hampering our understanding of the behaviour of such glaciers and the processes operating at their margins. During the Late Weichselian in West Iceland, an actively retreating marine-terminating glacier resulted in the large-scale deformation of a sequence of glaciomarine sediments. Due to isostatic rebound since the deglaciation, these formations are now exposed in the coastal cliffs of Belgsholt and Melabakkar-Ásbakkar in the Melasveit district, and provide a detailed record of past glacier dynamics and the interrelationships between glaciotectonic and sedimentary processes at the margin of this marine-terminating glacier. A comprehensive study of the sedimentology and glaciotectonic architecture of the coastal cliffs reveals a series of subaquatic moraines formed by a glacier advancing from Borgarfjörður to the north of the study area. Analyses of the style of deformation within each of the moraines demonstrate that they were primarily built up by ice-marginal/proglacial thrusting and folding of marine sediments, as well as deposition and subsequent deformation of ice-marginal subaquatic fans. The largest of the moraines exposed in the Melabakkar-Ásbakkar section is over 1.5 km wide and 30 m high and indicates the maximum extent of the Borgarfjörður glacier. Generally, the other moraines in the series become progressively younger towards the north, each designating an advance or still-stand position as the glacier oscillated during its overall northward retreat. During this active retreat, glaciomarine sediments rapidly accumulated in front of the glacier providing

material for new moraines. As the glacier finally receded from the area, the depressions between the moraines were infilled by continued glaciomarine sedimentation. This study highlights the dynamics of marine-terminating glaciers and may have implications for the interpretation of their sedimentological and geomorphological records.

Thorbjörg Sigfúsdóttir (thorbjorg.sigfusdottir@geol.lu.se), Department of Geology, Lund University, Sölvegatan 12, 223 62 Lund, Sweden and Institute of Earth Sciences, University of Iceland, Sturlugata 7, 101 Reykjavík, Iceland; Ívar Örn Benediktsson, Institute of Earth Sciences, University of Iceland, Sturlugata 7, 101 Reykjavík, Iceland; Emrys Phillips, British Geological Survey, The Lyell Centre, Research Avenue, Edinburgh, EH14 4AP, UK and Department of Geography, Queen Mary University of London, Mile End Road, London, E1 4NS, UK.

During the Last Glacial Maximum (LGM; *c.* 26.5-20 thousand years ago (cal. ka BP), Clark *et al.* 2009), major ice sheets around the globe expanded to reach the continental shelf break (Dyke *et al.* 2002; Hughes *et al.* 2016). During the following deglaciation, they commonly experienced multiple phases of re-advance and retreat leaving behind a complex sequence of glacially deformed (glaciotectonised) sediments and landforms (e.g. Harris *et al.* 1997; Williams *et al.* 2001; Phillips *et al.* 2002; Thomas & Chiverrell 2007). The sediments and structures present within these glaciotectonic landforms can often be directly related to processes occurring at the margin (proglacial) and beneath (subglacial) glaciers, thus shedding light on past ice sheet dynamics (i.e. Croot 1987; Bennett *et al.* 1999; Bennett 2001; Aber & Ber 2007; Benn & Evans 2010; Lee *et al.* 2013; Lee & Phillips 2013). Previous research on glaciotectonics has mostly focused on the structures associated with ice sheets and glaciers terminating in terrestrial settings (e.g. Bennett 2001; Bennett *et al.* 2004; Phillips *et al.* 2008; Lee *et al.* 2013), while relatively few studies have been performed on deformation related to marine-terminating glaciers.

Submarine landform systems formed at oscillating margins of marine-terminating glaciers have, however, been described from a number of locations within recently deglaciated fjords (Boulton *et al.* 1996, 1999; Ottesen & Dowdeswell 2006; Ottesen *et al.* 2008; Dowdeswell & Vásquez 2013; Flink *et al.* 2015), and associated with the terminal zones of retreating Weichselian ice sheets (e.g. Johnson & Ståhl 2010; Winkelmann *et al.* 2010; Ó Cofaigh *et al.* 2012; Johnson *et al.* 2013; Rydningen *et al.* 2013). Such landsystems commonly comprise large terminal moraines marking the maximum glacier extent, as well as streamlined landforms seperated by series of transverse ridges formed during still-stands or small readvances (Ottesen & Dowdeswell 2006; Ottesen *et al.* 2008; Winkelman *et al.* 2010; Flink *et al.* 2015). Less is known about the internal architecture of subaquatically formed moraines and therefore the glacial processes that caused their formation. The primary reason for this is the general lack of subaerial sections through moraines known to have formed on the sea floor. However, available sections through individual subaqueous moraines as well as published interpretations of offshore seismic data have shown that they have commonly been formed as a result of glaciotectonism (Sættem 1994; Seramur *et al.* 1997; Bennett *et al.* 1999; Johnson *et al.* 2013), and/or ice-marginal sedimentary processes such as gravity flows and the outflow of subglacial meltwater (Lønne 1995; Lønne *et al.* 2001; Lønne & Nemec 2011).

This paper contributes to the study of glacier-induced deformation at the margins of marine-terminating glaciers by examining the glaciotectonism recorded by the Late Weichselian glaciomarine sediments exposed in Melasveit, lower Borgarfjörður, western Iceland (Fig. 1A, B). Exposed in the coastal cliffs are a sequence of marine deposits showing evidence of deformation (ductile shearing, thrusting) by ice. The stratigraphy of these sediments has previously been described by Ingólfsson (1987, 1988), with the aim of reconstructing the regional glacial history. The present study adopts Ingólfsson's stratigraphic framework and focuses on the internal structural architecture of this well-developed submarine glaciotectonic complex. The intensity and style of deformation are interpreted in terms of episodic ice-marginal folding and thrusting during the active retreat of a glacier flowing from Borgarfjörður immediately to the north (Fig. 1A; Ingólfsson 1987, 1988; Norðdahl *et al.* 2008; Ingólfsson *et al.* 2010).

The study area and its geological context

Melasveit is a lowland area situated between the fjords Hvalfjörður and Borgarfjörður (Fig. 1A, B). To the northeast is the mountain range of Hafnarfjall and Skarðsheiði, its highest peaks rising to over 1000 meters above sea level (m a.s.l.) (Fig. 1A). The local bedrock is mainly composed of

Neogene basaltic lava flows, which crop out in the mountains and along the coast (Franzson 1978; Ingólfsson 1988).

Evidence for glacial activity is widespread in the region (Ingólfsson 1988; Norðdahl *et al.* 2008). The mountain landscape of Hafnarfjall – Skarðsheiði is characterised by trough-shaped valleys, horns and cirques formed as a result of repeated glaciations during the Pleistocene (Ingólfsson 1988). Striations on exposed bedrock surfaces show that, at some point, ice flowing down Borgarfjörður, Hvalfjörður and the Svínadalur valley coalesced in the lower Borgarfjörður region (Fig. 1A) (Ingólfsson 1988; Magnúsdóttir & Norðdahl 2000). The bedrock in Melasveit is blanketed by at least 30 m thick, dominantly glaciomarine deposits of Late Weichselian age (Ingólfsson 1987, 1988). This sequence is overlain by stratified sand and gravel thought to be of Holocene age, and records a major marine transgression following the final deglaciation of the area (Ingólfsson 1987, 1988). The most notable depositional glacial landform in the lower Borgarfjörður region is the Skorholtsmelar end moraine (Fig. 1B). This is a ~6 km long arcuate landform that rises ~20-40 m over its flat surroundings and has been interpreted as marking the maximum position of a Late Weichselian ice advance from Borgarfjörður (Ingólfsson 1988; Hart & Roberts 1994; Norðdahl *et al.* 2008; Ingólfsson *et al.* 2010). The exact age of this moraine is not known, but it has been suggested that it formed during the Younger Dryas (Ingólfsson 1988), late Bølling (Norðdahl *et al.* 2008; Ingólfsson *et al.* 2010) or possibly both (Ingólfsson 1988). The southern side of the moraine is flanked by deltaic deposits reaching up to 52 m a.s.l., which indicates the minimum relative sea level during, or following the moraine formation. On its northern side, i.e. at the ice-contact slope, the surface is littered with erratic boulders (Ingólfsson 1988).

The lower Borgarfjörður region, including the Melasveit area, likely became ice free in early Bølling, after a rapid collapse of an ice shelf off the west coast of Iceland (Ingólfsson 1987; Syvitski *et al.*

1999; Jennings *et al.* 2000; Norðdahl *et al.* 2008; Ingólfsson *et al.* 2010; Norðdahl & Ingólfsson, 2015). The collapse of this marine-terminating ice mass was most probably driven by a global rise in sea level resulting from the decay of other major northern hemisphere ice sheets (Ingólfsson & Norðdahl 2001; Norðdahl & Ingólfsson 2015; Patton *et al.* 2017).

The Melasveit area was submerged during most of the Late Weichselian, with the highest relative sea level occurring in the early Bølling, immediately after the deglaciation of the West Iceland shelf (Norðdahl *et al.* 2008; Norðdahl & Ingólfsson 2015). Raised marine shorelines, radiocarbon dated to 14.7 cal. ka BP, show that the relative sea level in the region was up to ~150 m higher than present (Ingólfsson & Norðdahl 2001; Norðdahl & Ingólfsson 2015). The subsequent marked decrease in the volume of ice covering Iceland during the remainder of the Bølling and into the Allerød (13.9-12.8 cal. ka BP) led to a rapid isostatic rebound and thus marine shore regression. Glacier expansion in the Younger Dryas (12.8 -11.7 cal. ka BP) caused renewed isostatic depression of the lower Borgarfjörður region and a rise in relative sea level of ~60-70 m. This led to the development of a younger series of raised marine terraces. During the Preboreal (11.7 -10.0 cal. ka BP), glaciers re-advanced leading to yet another isostatic depression and relative sea level rise in the region, up to ~65 m a.s.l. in the innermost part of Hvalfjörður (Fig. 1A; Norðdahl *et al.* 2008; Ingólfsson *et al.* 2010).

The locally deformed sequence of marine sediments, which are the focus of the present study, are now well-exposed in coastal cliffs due to the post-glacial isostatic uplift (Ingólfsson 1987, 1988; Norðdahl & Ingólfsson 2015). This provides a rare opportunity to study the interrelationships between glaciotectonics and sedimentation at the margin of a marine-terminating glacier. In most places such sequences remain concealed beneath the seabed.

127 Glaciotectonism observed in the coastal exposures in Melasveit has previously been attributed to an ice advance occurring shortly after 14.0 cal. ka BP, possibly as a result of the dynamic response of the western Iceland ice sheet following the earlier collapse of its marine-based component (Ingólfsson & Norðdahl 2001; Norðdahl *et al.* 2008; Ingólfsson *et al.* 2010). Furthermore Ingólfsson (1987, 1988) suggested another, more restricted, ice advance within the Younger Dryas based on stratigraphical evidence and radiocarbon dates.

Methods

The sedimentology and structural architecture of the Belgsholt and Melabakkar-Ásbakkar cliff sections (Fig. 1B-D) have been investigated using a range of macro-scale field techniques (Krüger & Kjær 1999; Evans & Benn 2004). The exposed sections were described in detail with particular emphasis being placed on recording the type of bedding, sediment type, bed geometry and structure (both sedimentary and glaciotectonic). The sediments were grouped into eight main sedimentary units (A-H) based upon lithofacies associations and other sediment properties, as well as their stratigraphical location. The terminology used for describing the glaciotectonic structures follows that normally used in bedrock structural geological studies (Phillips *et al.* 2011; Phillips 2017 and references therein). The geometry of folds, sense of displacement along thrusts and faults, as well as cross-cutting relationships between different sets of structures were systematically recorded. The orientation of fold axes, bedding, faults and joints measured in the field were plotted on a series of Schmidt equal-area lower hemisphere projections, and analysed using the Stereonet 9 software (Allmendinger *et al.* 2012; Cardozo & Allmendinger 2013). For ease of description, the Melabakkar-Ásbakkar cliffs were divided into several sub-sections, four of which were selected for more detailed analysis: Melaleiti, Ásgil, Ás-north and Ás-south (Fig. 1B). The sections are typically clean and free of surface debris due to the constant coastal erosion. As most of the cliffs are near-vertical only the lowermost parts could be accessed and examined in detail. The upper parts could only be approached at a few locations. The upper parts of the sections are thus mainly documented in the field using binoculars and by the detailed analysis of photomosaics and remotely sensed (LiDAR) images.

The Melabakkar-Ásbakkar cliffs and the Belgsholt section were scanned using a terrestrial, high-resolution RIEGL VZ1000 Light Detection and Ranging (LiDAR) Scanner in May 2014. The scanning was performed as a series of overlapping images spaced at 50-100 m intervals along the cliff sections. The position of the scanner was recorded using a differential Global Navigation System (dGNSS). After each scan, the relevant section of the cliff was photographed with a high resolution digital camera mounted on top of the scanner in order to apply the right colour to each scan point. The data from the scanner were processed in the RiSCAN PRO software package supplied by RIEGL in order to align and merge the scans manually. After the scans had been trimmed and aligned the data were exported into Bentley Pointools program for visualization and measurements. Analysis of the LiDAR images and photomosaics enabled the construction of detailed cross-sections through this variably glaciotectonised sequence.

The radiocarbon dates used in this study were previously obtained by Ingólfsson (1987) and calibrated by Norðdahl & Ingólfsson (2015) with the Marine13 calibration curve (Reimer *et al.* 2013) using the Radiocarbon Calibration Program (CALIB). The dates were reservoir corrected by 365±20 years ($\Delta R = 24\pm23$), which is the apparent age for living organism in the sea around Iceland (Håkansson 1983).

Sedimentology of the Late Weichselian to Holocene sedimentary sequence

The sediments exposed in the cliffs at Melasveit can be divided into eight major sedimentary units (A-H), which are often quite heterogeneous. In the undeformed parts of the sequence, these units typically occur in their correct stratigraphical order. However, large-scale thrusting associated with glaciotectonism has resulted in the localised repetition and/or excision of parts of this sequence. The individual sedimentary units are described below and their spatial distribution shown in Fig. 2.

Sediment unit A

This is the structurally and stratigraphically lowermost, and most widely exposed unit in the Belgsholt and Melabakkar-Ásbakkar cliff sections (Fig. 1B, 2). Its thickness ranges from 0 to ~25 m, measured from the base of the cliffs, but its lower contact is typically not exposed. An exception to this is at ~3000 m in the Melabakkar-Ásbakkar cliff (Fig. 2) where this unit rests directly on bedrock. The dominate facies within unit A is an extremely firm (hard), typically massive matrix-supported, greyish-brownish, silty-sandy diamicton which is locally rich in cobble-sized clasts (Fig. 3A). However, the characteristics of the diamicton vary along the cliffs. In the northern part of Melabakkar-Ásbakkar, most of the diamicton is heavily deformed, vaguely stratified and contains numerous irregular to lenticular-shaped sand intraclasts (up to several metres in length). Both the diamicton and sand intraclasts locally contain high concentrations of fragmented and occasionally intact mollusc shells (Fig. 3A). In the southern part of the Melabakkar-Ásbakkar cliff section, the unit A diamicton occurs interbedded with laterally extensive beds of poorly sorted sand, usually with irregular and gradational contacts. The sands locally contain small shell fragments.

Ingólfsson (1987) concluded that the mollusc fauna within unit A belong to the *Macoma calcarea* community, indicative of deposition in a low-salinity, shallow water, boreal - mid arctic fjord environment. Five radiocarbon-dated samples retrieved at different locations in the Melabakkar-Ásbakkar cliffs yielded ages ranging between *c.* 13.7 – 14.5 cal. ka BP.

Unit A sediments are interpreted as having been deposited in an ice-proximal to ice-distal marine setting, the sedimentary appearance most likely reflecting locally and temporally variable proximity to the ice margin at the time of deposition. The mollusc faunal assemblage within unit A is indicative of a shallow/near shore environment with a high input of freshwater or glacial meltwater (Ingólfsson 1987, 1988). The massive, structureless nature of the diamicton suggests deposition of fines from suspension with the inclusion of coarser clasts as ice-rafted debris (IRD). Although such sediments may possess a planar lamination due to the variation in sediment input over time, it may have been erased due to bioturbation by molluscs (e.g. Ó Cofaigh & Dowdeswell 2001). Furthermore the lack of distinct stratification may also have been partly caused by homogenisation due to post-sedimentary ductile deformation and liquefaction. The occurrence of interbedded sands suggests deposition in a more ice-proximal location, reflecting deposition from turbidity currents discharging from meltwater channels, deltas or outwash fans, causing winnowing of the sediments (Cowan *et al.* 1999; Boggs 2006). However, the locally high concentration of shells within the heterogeneous part of sediment unit A suggests deposition further away from the ice-margin where temperatures were higher, bioactivity also high and sediment accumulation rate lower (Powell & Molnia 1989; Powell & Domack 1995; Jaeger & Nittrouer 1999; Ó Cofaigh & Dowdeswell 2001).

Sediment unit B

Unit B sediments are exposed at Belgsholt and at a few places within the Melabakkar-Ásbakkar cliffs, most notably between ~1600-2800 and 3300-3700 m (Fig. 2). This unit has an undulating geometry and its thickness is highly variable laterally with the thickest parts (>15 m) being exposed at Melabakkar-Ásbakkar between ~3400-3800 m. The dominant facies comprises alternating beds of well sorted coarse to fine sand and cobble gravel beds, as well as frequent interbeds and lenses of massive fines (silt/fine sand) and silty-sandy diamicton (Fig. 3B, 3C). The diamicton layers/lenses within unit B are most prominent at Ás-north (Fig. 2, ~3600-3800 m) where they are up to ~3 m thick. The planar and trough-cross bedded sand and gravel beds are laterally discontinuous with erosive bases, the thickness of individual beds ranging from centimetres to over a meter. Unit B sediments are typically sheared, folded and faulted, except between 2600- 2800 m (Fig. 2) where they form an up to 15 m thick sequence of undeformed coarse, well-stratified gravel with subrounded to well-rounded pebble to boulder-sized clasts (Fig. 3C). Some beds contain a large amount of mollusc fragments with abraded edges; no whole, un-abraded shells were detected. The lower contacts of unit B are only exposed between 1600-1700 and 3500–3900 m (Fig. 2) where unit B overlies sediment unit A, and between ~2300-2400 where it rests upon sedimentary unit D (see below). The contacts of unit B with these other sediment packages frequently show evidence of shearing and tectonic mixing with the structurally underlying sediment units.

The sedimentary structures, large grain sizes, sorting and roundness of clasts, as well as a high content of shell fragments suggest that the sands and gravels of unit B were deposited from meltwater discharge in a relatively high energy, marine environment. This type of environment frequently occurs at the margin of marine-terminating glaciers where coarse-grained sediments are brought into the ocean by subglacial meltwater streams (Powell & Molnia 1989; Powell & Domack 1995; Powell 2003). The massive, fine-grained sediment layers that interdigitate with the sorted sand and gravel may represent debris flows and/or fallout from suspension, both of which are common processes in ice-contact marine systems (Powell & Molnia 1989; Lønne 1995; Powell 2003). The shell fragments are likely to be reworked and therefore do not reflect the faunal assemblage living at the time of sediment deposition.

Sediment unit C

Unit C sediments are exposed between ~3000 and 3500 m at Melabakkar-Ásbakkar where they range from 1- 20 m thick and unconformably overlie units A and B (Fig. 2). The dominant facies comprises planar and cross-laminated fine sand interbedded with massive silt. This sand and silt sequence is unconformably overlain by a massive silty-sandy and relatively clast-poor diamicton (Fig. 3D). The sediments of unit C have been subject to both ductile and brittle deformation immediately below the diamicton. No shells or shell fragments were found in the lower interbedded part of the sequence, while small fragments were observed in the diamicton.

The dominance of fine-grained laminated silts and sands with occasional outsized clasts suggests deposition in a glaciomarine setting in which the massive silt beds were deposited from suspension settling, while planar and cross laminated sand formed from turbidity currents (Powell & Molnia 1989; Ó Cofaigh & Dowdeswell 2001). The absence of in situ mollusc shells suggests a hostile environment, either due to low temperatures and/or high sedimentation rate (Ó Cofaigh & Dowdeswell 2001). The diamicton in the upper part of unit C is interpreted as a mass flow deposit (Nichols 2009; Ó Cofaigh & Dowdeswell 2001) containing reworked shell fragments. Emplacement of this mass flow is thought to have resulted in the observed disruption of the underlying silts and sands . Alternatively, the diamicton could be interpreted as a subglacial traction till deposited at the ice-bed interface. During its emplacement, the underlying unit C sediments may have been subjected to glaciotectonic deformation.

Sediment unit D

This sediment unit is up to ~25 m thick and was observed in the Melabakkar–Ásbakkar cliffs between ~600-700 m, 1600 and 2600 m, as well as within the southernmost part of this section between 4700-5000 m (Fig. 2) . The dominant facies is a poorly sorted, massive fine sandy silt, often with bed thickness over one meter, separated by much thinner (cm scale) beds of medium to coarse sand (Fig. 3B). Occasional pebble-sized clasts (up to a few cm) are found dispersed within the silt beds. The sediments of unit D are deformed and locally appear to have been homogenised to form a fine-grained, clast poor diamicton. Unit D sediments have locally been thrust over unit B (e.g. Fig. 3B). The glaciotectonic contact between units B and D is irregular, and shows evidence of both brittle faulting and ductile shearing, as well as liquefaction and mixing between these sedimentary units (see below). A few small mollusc fragments (mm scale) were found, mostly in the lowermost parts of unit D, but no whole mollusc shells or larger fragments were detected. Ingólfsson (1987) has published three radiocarbon dates on shell fragments collected at ~2550 m (Fig. 2) that range in age between *c.* 13.4-13.5 cal. ka BP. This suggests a maximum age of sediment deposition was during the Allerød.

Sediments of unit D are interpreted as having been deposited in an ice-proximal glaciomarine environment. The thick beds of massive sandy silt represent deposition by suspension settling from buoyant meltwater plumes and the pebble intraclasts deposited by means of debris rain-out from icebergs (Powell & Molnia 1989; Lønne 1995). The mollusc fragments are clearly redeposited, their age only giving a maximum age of sediment deposition. The absence of whole shells suggests a too hostile environment for mollusc fauna, possibly reflecting a high rate of sediment accumulation (Ó Cofaigh & Dowdeswell 2001).

Sediment unit E

Unit E sediments are exposed between ~10-100 m in Belgsholt (Fig. 2) where it is up to ~6 m thick, and in Melabakkar-Ásbakkar section at ~0-300 m (Fig. 2) where at Melaleiti the unit is 8 m thick. The dominant facies comprises beds of well-sorted, both planar cross-bedded and planar laminated medium-grained sand, alternating with beds of massive silt. Bed thicknesses are generally in the cm- to dm-scale. In the lower part of unit E are occasional beds of gravel (bed thicknesses in the order of centimetres) and beds of sandy silty diamicton (up to ~1 m thick); the latter containing small mollusc fragments. The contacts between the beds of different facies are typically sharp and erosive, with the sand beds commonly containing silt intraclasts which are lithologically similar to the interbedded massive silts, indicative of localized penecontemporaneous erosion.

The appearance of the sediments within unit E varies along the cliff section. At Belgsholt, the sand and silt beds in the lowermost part are up to few dm thick and commonly exhibit small scale synsedimentary folds and overturned flame structures. The beds become thinner and less deformed upwards and in the uppermost ~3 m they contain abundant intact mollusc shells; identified species are *Balanus balanus, Buccinum undatum, Hiatella arctica and Macoma calcerea*. At the Melaleiti section there is no obvious vertical variation in bed thickness or grain size of unit E sediments. Synsedimentary folds and flame structures up to 50 cm in amplitude are common (Fig. 3E). At Belgsholt, the contact between unit E and units A and B is tectonic, while at Melaleiti the boundary between units E and A ranges from sharp to gradational.

The alternating planar and cross laminated sand with beds of massive silt suggests deposition from turbidity currents alternating with suspension settling of fine grained sediments from meltwater plumes (Ó Cofaigh & Dowdeswell 2001). The flame structures are most likely a result of loading of water-saturated mud, with the resultant water-escape leading to the deflection upwards of the interbedded sand layers. The presence of these water-escape features within unit E is consistent with high rates of sedimentation. The loading was most likely accompanied by mass movement, leading to the overturning of the load structures in the direction of emplacement of the mass-flow (Boggs 2006). The diamicton beds in the lower part of unit E are thought to represent subaqueous sediment gravity flows with their emplacement having been accompanied by localized soft-sediment deformation (Lønne 1995; Boggs 2006). Together, this suggests a high energy, unstable, depositional environment located close to the ice margin, while the upward fining trend, as well as the marine fauna, in the upper beds of unit E at Belgsholt suggests a progressively increasing distance from the ice front during deposition of unit E; potentially recording the retreat of the ice front. The marine fauna observed at Belgsholt indicates shallow coastal water and the presence *Buccinum undatum*, which is a subarctic species (Símonarson 1981), relatively warm water temperatures.

Sediment unit F

Unit F sediments were observed in the northern part of the Melabakkar-Ásbakkar cliffs between 0 – 2800 m (Fig. 2). The dominant facies is a massive clast-supported gravel with sub-rounded to rounded clasts and with a sandy matrix infill. Maximum particle size is generally around 0.5 m, although occasionally larger clasts, up to ~2 m in diameter, also were found. Unit F forms a thin (maximum thickness ~3 m) and undulating bed following the shape of the underlying topography. Its lower contact is erosional, especially between 1000 - 1600 m, where the clast sizes also tend to be their largest (Fig. 3F). Sediment intra-clasts which are clearly derived from underlying sedimentary units A and D are common within unit F. The southward tilted rip-up structures show palaeocurrent direction towards the south. No mollusc shells were observed in the sediment.

The clast roundness, erosional lower contacts, as well as the large particle sizes, suggest sedimentation by running water in a high-energy environment. Massive boulder beds and lag deposits similar to those of unit F which contain frequent rip-up clasts due to erosion of underlying beds have been described in glacial outburst flood (jökulhlaup) deposits in Iceland (Maizels 1997; Marren 2005). The fact that unit F follows the undulating surface topography of underlying sedimentary units suggests that it was deposited under high pressure in a confined space where the fluid flow followed the topography of the substratum instead of accumulating in depressions, as would be expected in an unconfined setting. Based on this, unit F is interpreted as having been deposited at the ice/bed interface by pressurised subglacial meltwater flows. Similar coarse-grained sediments with erosive bases, argued to be diagnostic for subglacial excavation and deposition in subglacial cavities during high-energy flow conditions have been described from Skeiðarárjökull on Iceland (Russell *et al.* 2006).

Sediment unit G

Unit G sediments are exposed at a few places within the Melabakkar-Ásbakkar cliff, most notably between 300-600, 900-1600 and 2500-3200 m (Fig. 2), and within the Belgsholt cliff section (between ~100-250 m; Fig. 2). It is undeformed, draping the topography of the underlying sediment units and is separated from these variably deformed sediments by a sharp contact (Fig. 3C, D, F). Although Unit G records an overall upward fining trend. The lower part of the unit mainly consists of relatively thick beds of interbedded diamicton and sand (often >1 m thick beds) as well as local occurrences of thin gravel beds (cm- or dm- scale), with erosional contacts. The silty-sandy diamicton beds are usually massive, while the sand beds show both planar and cross lamination. Evidence of soft-sediment deformation, such as convolute bedding and flame, ball and pillow structures, are commonly found within individual beds in the lower part of the unit. The upper parts of unit G commonly consist of planar laminated silt and fine sand. No mollusc shells were found within unit G.

The diamicton beds which dominate the lower part of unit G are interpreted as deposited from high-density sediment gravity flows, common in ice-contact environments due to instable slopes, high sedimentation rates and calving (Powell & Molnia 1989; Lønne 1995; Boggs 2006). The interbedded planar to cross-bedded sands are thought to record traction deposition from more diluted sediment underflows. The soft-sediment deformation structures within these beds is indicative of fast sediment deposition resulting in localised liquefaction and water-escape. The absence of mollusc shells may also indicate high sedimentation rates, although it is also possible that this absence is due to unfavourable temperature conditions (Ó Cofaigh & Dowdeswell 2001; Boggs 2006). Measured depositional rates in front of contemporary retreating glacier margins in Alaska, Greenland and Svalbard are reported to be as high as several decimetres per year (Cowan *et al.* 1999; Jaeger & Nittrouger 1999; Gilbert *et al.* 2002; Trusel *et al.* 2010). The change in lithofacies upwards within unit G to a sequence dominated by laminated silt and fine sand suggests a progressive lowering of energy levels and increased distance from the sediment source, reflecting retreat of the ice margin. Sedimentation in the upper part of the sequence is thought to have been dominated by suspension settling of fine sediments out of a buoyant sediment plume (Ó Cofaigh & Dowdeswell 2001).

Sediment unit H

Unit H constitutes the stratigraphically youngest part of the sedimentary sequence and can be traced laterally along the entire Melabakkar-Ásbakkar section, and corresponds to the uppermost part of the succession identified by Ingólfsson (1987). Unit H ranges in thickness from ~10 m at 0-400 m to ~1 m in most places beyond 3000 m. This sedimentary unit is generally separated from the underlying units by a distinct unconformity (erosion surface). The dominant facies within unit H is horizontally bedded sands and gravels which define an overall coarsening upwards sequence.

However, in detail these sediments also exhibit smaller-scale changes in grain size both vertically and laterally. For example at ~300-400 m, the unit consists of cross-bedded gravel, whereas at ~500-700 m it comprises a 6 m thick sequence of planar and cross-laminated sand with occasional load structures. No detailed examination of unit H could be performed because of inaccessibility at the top of the cliffs.

Unit H sediments have previously been interpreted as comprising a complex, time-transgressive sequence of beach (littoral zone) sediments and aeolian sand which were formed during a marine regression and emergence of the landscape in the early Holocene (Ingólfsson 1987, 1988).

Structural architecture of Belgsholt and Melabakkar-Ásbakkar

The detailed internal structural architecture of the Belgsholt and Melabakkar-Ásbakkar sections are described below and illustrated in Fig. 2.

Belgsholt

The northernmost section, Belgsholt, occurs in an elongated, E-W trending ridge, situated approximately 500 m north-east of the main Melabakkar-Ásbakkar cliff section (Fig. 1B). The ridge is cut by a transverse ~250 m long, N-S oriented, 12 m high subvertical coastal cliff (Fig. 4A). The northernmost ~100 m are clean and free from surface debris enabling a detailed examination of the internal architecture of the ridge. The remainder of the cliff section is partly obscured by surface wash and debris.

Structural architecture. The Belgsholt section can be divided into two parts based on the style and relative intensity of deformation; (i) the northern part (0-110 m; Fig. 4A) characterised by the presence of a large syncline-anticline pair affecting units B and E and (ii) the southern part (110-250 m; Fig. 4A), which consists of undeformed laminated sediments (unit G) overlying deformed sand and diamicton (unit A and B).

The sediments in the northern part of the section (0-110 m) are dominated by the interbedded silts and sands of unit E, resting upon the bedded sands and gravels of unit B. At this locality, the base of unit E is poorly defined and deformed with the small-scale folds along this boundary indicating that it has been modified by bedding-parallel shearing. The dominant deformation structure in the section is a large-scale syncline-anticline pair (~50-100 m; Fig. 4A). The syncline is upright with amplitude over 12 m and wavelength ~40 m with its axis plunging 4° to the ESE (Fig. 4B). Bedding-parallel shearing appears to have occurred prior to the folding as the tectonised contact between units E and B is folded by the syncline. The bedding within the core of the fold is offset by numerous, steeply inclined reverse faults (displacement in the order of cm or dm) that fan around the axis of the syncline (Fig. 4A, B). These faults have sharp planes and extend outwards to deform the structurally underlying stratified sand and gravels of unit B. Although deformed, primary sedimentary structures and relationships between the beds within unit E are well preserved. Between 70 and 100 m, the unit B sands and gravels occur within a south-verging anticline (Fig. 4A, C). Primary sedimentary features within the core of the anticline have been overprinted during deformation and the sand has been homogenized by liquefaction. The limbs of the anticline are cross-cut by minor faults (displacement of only mm to few cm), mainly reverse faults, developed approximately orthogonal to the bedding surfaces.

The sequence exposed in the southern part of the Belgsholt section (110-250 m) is composed of the massive/heterogeneous silty-sandy diamicton (unit A) overlain by stratified sand and gravel (unit B). These lithofacies associations are interfingering and show evidence of soft-sediment deformation; probably as a result of syn-sedimentary compaction and loading of still wet sediments. Immediately adjacent to the south-verging anticline (between 90 and 110 m; Fig. 4A) both units A and B show evidence of locally intense, and highly disruptive, ductile deformation and associated liquefaction, and also contain a large number of intraclasts (individual clasts over 1 m in diameter) of sand. Relatively undeformed beds of silt and sand (unit G) unconformably overlie the deformed sequence from ~90 m southwards and the whole sequence is truncated by a horizontally bedded gravel unit (unit H).

Structural evolution. The relatively simple internal architecture of the Belgsholt ridge is consistent with lateral (sub-horizontal) compressive deformation, as a result of ice-push from the north/north-east. The south-verging syncline-anticline fold pair is interpreted as recording ductile folding as the ice advanced into the pre-existing marine sediments. Minor brittle faulting of the sediments within units B and E occurred as the sequence accommodated further compression imposed by the advancing ice.

The focusing of ductile deformation along the lithological boundary between unit E and the structurally underlying sands and gravels of unit B may simply reflect the marked lithological/rheological contrasts between these two units. This deformation probably occurred during the onset of glaciotectonic deformation at Belgsholt (i.e. prior to folding) and possibly records the earliest stages of shortening of the sediment wedge in response to initial ice-push. As the ice continued to advance, this tectonised boundary was folded into the upright syncline which dominates the northern part (Fig. 4A, B). Alternatively, this sheared boundary may represent an earlier formed, bedding-parallel thrust resulting from the southerly transport of a detached slab of unit E sediments and its emplacement upon the sands and gravels of unit B.

The relative intensity and complexity of the deformation observed in the northern part of the Belgsholt section initially increases southward towards the central part of the section (~50-100 m), before fading out in the remaining part of the section (Fig. 4A). The sediments deformed by the south-verging anticline and immediately south of this fold show evidence of soft-sediment deformation and liquefaction (Fig. 4A, C). The fluidised sediments were remobilized and injected upwards in the form of diapirs and clastic dykes. There is no definitive evidence that the advancing ice overrode the sequence at Belgsholt (e.g. evidence for subglacial shearing): therefore, the diapirs and clastic dykes may simply be recording the escape of pressurized meltwater from the deforming sequence driven by a hydrostatic pressure gradient formed by the weight of the advancing ice. Compression of wet sediments immediately in front of the advancing ice mass would have resulted in an increase in porewater pressure leading to liquefaction and injection of the remobilized sediments. Localized faulting of the sediments observed cutting through the diapirs and clastic dykes within units A and B indicates that deformation continued after liquefaction, consistent with dewatering of the sediments prior to the termination of glaciotectonic deformation.

Although the Belgsholt ridge has most likely undergone some erosion since its formation, the location of the most highly deformed part of the sequence below the crest line suggests that the ridge is a morphological expression of the glaciotectonics below. This is further supported by the structural reconstructions indicating ice movement from the north, approximately perpendicular to the trend of the ridge. Based on this association between the ridge morphology and the compressional nature of the glaciotectonics, as well as the localized nature of the deformation, the ridge is interpreted as an ice-shoved ridge (e.g. Aber & Ber 2007). The deformation is mostly confined to the proximal (northern) and central part of the ridge which indicates that the former ice margin was located on the northern side of the ridge.

Melaleiti

The Melaleiti structural zone occurs at the northern end of the Melabakkar-Ásbakkar coastal cliffs, between 0 and 300 m (Fig. 2). At Melaleiti, the cliff is oriented NNE-SSW and rises vertically up to 30 m a.s.l. The cliff face is mostly dry allowing a detailed documentation of the sedimentary features and glaciotectonics. Bedrock outcrops are found at sea level just north of the section and ~100-200 m offshore.

The stratigraphy at Melaleiti can be divided into three main structural units (Fig. 5A): i) The deformed sequence which dominates the lowermost ~13 m of the cliff section and forms the Melaleiti structural zone (units A and E); ii) an undulating gravel bed (unit F) overlain by a sequence of alternating silt, sand and clast poor diamicton (unit G); and iii) the structurally higher Holocene sequence of littoral sediments (unit H; Ingólfsson 1987, 1988).

Structural architecture. The Melaleiti structural zone consists of sub-horizontal to gently northwards tilted, thrust-bound blocks comprising the silty-sandy diamicton of unit A and interbedded silts and sands of unit E.

In the northern part of the section (~0- 80 m; Fig. 5A) the thrust blocks are separated by a poorly defined, undulating shear plane. Internally, the thrust-bound blocks are pervasively deformed showing evidence of homogenisation due to ductile deformation and the contacts between the internal sediments (units A and E) are generally diffused. They are dissected by a series of southeast dipping normal (extensional) faults, as well as some smaller scale steep, northwest dipping, reverse and normal faults (Fig. 5A). These faults seem to be truncated by and therefore predate the shear plane. The displacement on both sets of faults is generally in the order of centimetres or decimetres. Most of the faults are undulating and commonly infilled/lined by massive, fine-grained sediments which suggests that they acted as fluid pathways.

The middle part of the section (80-110 m; Fig. 5A) exhibits the most complicated deformation in the Melaleiti zone. The most notable structures in this part are a number of southeast dipping shear planes which break up the thrust blocks of units A and E into a series of northward dipping fault blocks. The fault blocks and the shear planes are cross-cut by undulating open, southward dipping fractures that are infilled by massive sand-rich sediments. The shear planes are poorly defined and are frequently lined by deformed, fine-grained sediments. Although hard to estimate, the offset of internal bedding within unit E suggests that the displacement might be a few meters towards the southeast.

The southern part of the Melaleiti section (110-250 m; Fig. 5A) exhibits somewhat simpler and less penetrative deformation than the northern part. A gently northward dipping discrete shear plane divides the sequence into two thrust blocks, each containing both units A and E. Although deformed, internal sediment features within unit E in both upper and lower thrust block are easily recognizable and can be traced throughout a large part of this structural unit. However, the sediments immediately below the shear plane show evidence of intense ductile deformation (shearing and folding) which decreases in intensity and depth of penetration towards south (Fig. 5A-D). The sediments in the footwall of this shear plane are cut by numerous reverse and normal faults (Fig. 5C, D). The dominant fault type varies laterally; in particular most of the faults between 100 and 150 m are north-dipping reverse (compressional) faults, whereas between ~180 and 300 m the faults are mainly extensional (normal) dipping both towards southwest and northeast (Fig. 5A). Most of these faults only cut through the footwall although a few cross-cut and therefore postdate the thrust boundary and extend upwards into the hanging wall (Fig. 5A, D). Some of the faults are infilled by sand suggesting that these may have acted as fluid pathways (hydrofractures) (Rijsdijk *et al.* 1999; Phillips & Merritt 2008; van der Meer *et al.* 2009; Phillips & Hughes 2014). The upper block forms a large boudinage structure between 170 and 250 m (Fig. 5A, C).

Structural evolution. The overall structural architecture of the Melaleiti section indicates a thrust zone where blocks composed of the marine diamicton of unit A and interbedded sands and silts of unit E have been thrusted and stacked as a result of sub-horizontal compressional deformation (Fig. 6). Such thrust-stack sequences generally form in an ice-marginal or proglacial position due to gravity spreading and compression from the rear by the forward movement of the ice (e.g. Aber *et al*. 1989; Bennett *et al.* 1999; Boulton *et al.* 1999; Bennett 2001; Pedersen 2005; Phillips *et al.* 2008, 2017; Benediktsson *et al.* 2010, 2015; Benn & Evans 2010). Based on the configuration of these thrust blocks and orientation of faults, this deformation was caused by an ice-push from the northwest (Fig. 5A). The overall decrease in strain from north to south can therefore be explained by decreasing amount of stress transferred from the source of tectonic pressure, i.e. an advancing ice margin, towards the foreland.

Shear zones like the one separating the thrust-blocks at the southern part of Melaleiti are commonly found below glacially transported sediment rafts where the displacement is facilitated by a thin water-lubricated detachment (e.g. Benediktsson *et al.* 2008; Phillips & Merritt 2008). Vaughan-Hirsch *et al.* (2013) argue that elevated porewater pressures during glaciotectonism can lead to liquefaction of the sediments within the shear zone, lowering their cohesive strength and thereby aiding forward movement of the overriding thrust block. Therefore, based on the nature of contacts, the detachment and transportation of the thrust sheets at Melaleiti is thought to have been facilitated by elevated porewater pressures during glaciotectonism. The tectonic thickening may have caused a build-up of porewater pressures within the developing thrust stacks leading to hydrofracturing when the pressure exceeded the cohesive strength of the sediments and the depressurization of the lubricated detachments (Rijsdijk *et al.* 1999; Phillips & Merritt 2008; Rijsdijk *et al.* 2010). Subsequently the forward movement of the thrust sheets was accommodated by extensional deformation in the lower thrust sheet causing the formation of normal faults. The sediments became increasingly well drained towards the distal (south) part of the moraine reflected by the better defined fault/fracture planes towards the south. Similar pattern of the continuing brittle deformation after a fall in porewater pressures are known from both modern and past glacial environments (e.g. Benediktsson *et al.* 2008, 2010; Phillips & Merritt 2008). The thrust blocks are draped by the subglacial gravel of unit F showing that the zone was overridden by a glacier after the ridge was formed. This may have resulted in further extensional deformation of the thrust stacks, such as the boudinage structure of the upper thrust block (between 150 and 250m; Fig. 2) and a set of extensional faults dissecting the thrust blocks and the boundary between (Fig. 6).

Fúla Bay

The Fúla Bay comprises several sub-zones occurring between 400 and 2000 m (Fig. 2). The overall architecture of these zones is only briefly described because a detailed investigation was hampered by overhangs and frequent rock falls as well as water and thin debris cover on the cliff face.

Structural architecture. The structural zones in Fúla are mostly composed of the deformed sediments of units A, B and D. The deformed units A and D as well as local occurrences of unit B in between form a small number of ridges, the two largest of which are up to 30 m high (at 600-900 and 1300-2000 m; Fig. 2). The architecture of the ridge at 600-900 m indicates that it comprises stacked, thrust blocks dipping into the northwest (ranging 276-316°; Fig. 7). Numerous normal faults with a down-throw to the south (ranging 156-216°; Fig. 7) were identified in the lowermost parts of the ridge (Fig. 2). However, it was typically not possible to determine the amount of fault displacement or how far up the sequence the faults extended. The ridge between 1300-2000 m mainly consists of apparently subhorizontally bedded unit D resting upon heavily deformed units A and B. The most part of unit D, however, is only weakly deformed although the lower contacts are sheared, folded and dissected by numerous compressional and extensional faults (Fig. 2).

The coarse gravel and boulder bed of unit F, interpreted as a subglacial deposit that caps the deformational zone at Melaleiti, can also be traced along the entire Fúla zone (Fig. 2, 3F). The gravel follows the ridge-like topography of the deformed unit A below and is equally thick on the ridge crests as in swales between the ridges.

Structural evolution. The zone located between 600 and 900 m comprises a thrust-stack sequence indicating that it was formed by a sub-horizontal, compressional deformation in an ice-marginal or proglacial position (Bennett *et al.* 1999; Boulton *et al.* 1999; Bennett 2001; Phillips *et al.* 2008, 2017; Benn & Evans 2010). The orientations of the thrust sheets and faults suggest an ice-flow from the northwest (Fig. 7). The lower contacts of unit D within the structural zone between 1300-2000 m is interpreted as a thrust boundary based on the shearing and folding concentrated along the contacts. Although no structural measurements could be carried out in this part of the cliffs, it is likely, that the glaciotectonic stress direction was also from the north/northwest. Between 1600-2000 m the cliff is orientated E-W, approximately perpendicular to the main glaciotectonic stress direction, making the beds to appear horizontal in the cliff wall. The presence of the subglacial gravel of unit F on top of all the ridges in the Fúla Bay indicates that they were overridden and perhaps also eroded and reshaped by a glacier after the thrust stacks were formed. The southward dipping faults detected within the Fúla structural zone (Fig. 7) might have been developed in response to this subglacial modification.

Ásgil

The Ásgil structural zone is located in the central part of the Melabakkar-Ásbakkar cliffs, north of the Ásgil gully, between ~2250 and 2600 m (Fig. 2, 8A). The cliff face at this site is sub-vertical and oriented northwest-southeast. The southern part of the section is mostly clean and well exposed allowing detailed documentation of deformation structures, whereas the northern part (2250-2400 m; Fig. 8A) is partially concealed by surface wash and debris.

Ásgil can be divided into three main structural units: i) the deformed zone comprising stratified gravel of unit B and interbedded silts and sands of unit D. These deformed sediments rest on unit A which is not exposed in the cliffs but can be seen on the foreshore at low tide; ii) The interbedded unit G, which overlaps the underlying deformed units; and iii) the uppermost Holocene sequence of littoral gravels (unit H).

The Ásgil deformed zone is divided into two parts based on the style of deformation; (i) the northern part (2250-2400 m, Fig. 8A), which is dominated by large-scale folds and (ii) the southern part (~2400-2700 m, Fig. 8A), which is characterized by stacked, northward dipping thrust blocks.

Ásgil north - structural architecture. The northern part of the Ásgil section (2250-2400 m; Fig. 8A) is characterized by a few upright to gently northward verging folds which become progressively tighter towards the southeast with amplitudes of up to about 20 m and deform the ice-marginal sand and gravel of unit B and the silts and sands of unit D.

The northernmost fold is an open syncline (2300-2330 m; Fig. 8A), followed by a closed anticline at 2330-2350 m (Fig. 8A). They both appear to have fold axes trending approximately southwest-northeast based on measurements from the southeastwards dipping fold limb. Two or three tight/isoclinal folds are also found at ~2350 m (Fig. 8A). Despite being deformed, primary sedimentary structures (e.g. bedding) are usually well-preserved within the sands and gravels of unit B. The folds are dissected by a number of fractures and minor faults (displacement in the order of mm to cm), many of which seem to radiate from the centre of the folds (Fig 8A; ~2300-2350 m). Based on the stratigraphy and the proximity to the southernmost thrust zone at Fúla Bay (1300-2000 m; Fig. 2) these are interpreted to be part of the same structural zone.

Ásgil north-structural evolution. The large folds present in the northern part of the section (at ~2250-2400 m; Fig. 8A) most likely post-date the southern-part as it doesn't show any indications of being overprinted by stress from the northwest (high relief and a lack of overturning) and the sediments affected by the folding appear to structurally overly the deformation zone at Ásgil-south. The folds might be glaciotectonic, possibly representing proglacial deformation formed as the ice was forming the thrust stacks observed south of the zone at Fúla Bay (1300-2000 m; Fig. 2). Alternatively, they could have formed during slumping in response to large-scale gravity flows as the glacier retreated from the area (Boggs 2006). The radiating geometry of most of the faults dissecting the folds suggests that these were developed in response to horizontal shortening of the sediment as it was folded.

Ásgil south - structural architecture. The most notable large-scale structures at the southern part of Ásgil (2400-2650 m; Fig. 2) are a number of stacked, convex upward thrust-bound blocks of the silts and sands of unit D (Fig. 8A). Measurement of the lowermost block shows that it dips towards the north (Fig. 8A). Internally unit D exhibits deformation structures indicative of shearing, apparently from a northerly direction (e.g. folds and augen structures; Fig. 8B).

The lowermost thrust block rests on the sub-horizontally bedded sands and gravels of unit B. The level of internal deformation within unit B changes laterally. Between 2450 and 2550 m (Fig. 8A), unit B is heavily folded and the boundaries between units B and D are interfingering and diffused. A number of fractures and minor faults, with a displacement usually in the order of millimetres or centimetres, cross-cut the silts and sands (unit D), and the sands and gravels of unit B (Fig. 8A, B). The deformation gradually becomes less penetrative southward and at the southernmost part of the section most of the sands and gravels of unit B show little or no evidence of deformation. However, in this area the boundaries between unit B and D are defined by a thin and highly distorted zone (~50 cm) of layered clay, silt and gravels (Fig. 8C). This zone is locally offset by both small and large-scale faults and fractures (Fig. 8A, D), including a set of steeply inclined, southeast dipping open fractures consistent with water-escape structures/hydrofractures formed by the escape of pressurized water under or in front of ice margins (Rijsdijk *et al.* 1999; Kjær *et al.* 2006; Benediktsson *et al.* 2008; van der Meer *et al.* 2009). These hydrofractures extend upward into unit D. They are up to a few meters long and their widths are in the order of centimetres and are infilled by massive and sorted sediments, mainly sand and fine gravel (Fig. 8D). The sediment infillings of some of these fractures exhibit various sedimentary structures typical of fluid transport, such as planar parallel-bedding and cross-bedding.

The stratified sand and gravel (unit B) continues at the other side of the Ásgil gully. It is unconformably overlain by a coarse gravel and together they form up to 15 m high and 200 m long multi-crested pile of well-bedded, sorted sand, gravel and boulder gravel of unit B (Fig. 2, 3C). The inclined bedding (foresets) within the unit is consistent with apparent palaeoflow direction towards the southeast. Primary sedimentary structures such as planar- and trough-cross beddings are intact and there are no or signs of glaciotectonic deformation.

Ásgil south - Structural evolution. The structural architecture of the southern part of the Ásgil section comprising northward dipping thrust stacks is consistent with its formation in response to thrusting and compressional deformation (Fig. 9) (i.e. Bennett 2001; Benediktsson *et al.* 2008, 2015; Pedersen 2014; Phillips *et al*. 2017). Based on this, the Ásgil zone is interpreted as an ice-marginal/proglacial moraine deposited by a glacier advancing from the north (Boulton *et al.* 1999; Bennett 2001). This was accompanied by release of glacial meltwater and the deposition of the ice-marginal sands and gravels of unit B both before and after the termination of the glacial advance.

The highly deformed boundary between units B and D (Fig 8A; ~2450-2600m) provides evidence for displacement of the lowermost block along this interface indicating that the thrust blocks of unit D partially overrode the ice-marginal sediments of unit B. This would have caused elevated porewater pressures in the ice marginal sands and gravels in response to the thickening of the thrust stack causing liquefaction, hydrofracturing and injection of sand and gravel into the base of the lowermost thrust block (Rijsdijk *et al.* 1999; Kjær *et al.* 2006; Benediktsson *et al.* 2008; van der Meer *et al.* 2009). The localized faulting of the sediments further indicates that some minor deformation continued after the sediments had been drained.

The large accumulation of coarse sand and gravels of unit B, at the southern (distal) end of the zone show very little signs of deformation. These sands and gravels are interpreted as subaquatic fan and were most likely formed as the ice margin stood still after the cessation of the advance (Fig. 9). As it is undeformed it shows that the area did not experience further glacial pushing or overriding after the moraine was formed.

Ás

The Ás structural zone is located in the Melabakkar-Ásbakkar cliffs between ~3400 and 5000 m (Fig. 2), which makes it the largest of the structural zones in the entire cliff section and the only structural zone that does have a clear morphological expression. A detailed analysis was carried out in two separate parts of the Ás structural zone; the northern part at 3500-3700 m (Fig. 2) and the southern part at 4500-5000 m (Fig. 2). These parts are called Ás-north and Ás-south, respectively. The cliff face between these two parts (at 3800-4500 m; Fig. 2) was largely obscured due to surface wash and debris cover. However, large-scale folds and northward dipping thrusts could be identified through the surface wash, clearly showing that this part of the cliff is also deformed.

Ás-north - structural architecture. The cliff face at Ás-north is sub-vertical and is oriented NW-SE (326°-146°). The northern part of the section is ~23 m high, mostly clean and well-exposed, allowing a detailed examination whereas the lowermost ~10 m of the southern part (3575-3680 m; Fig. 10A) is covered in surface wash and debris.

The stratigraphy at Ásgil can be divided into three main structural units: i) the deformed zone comprising the silty-sandy diamicton of unit A and the stratified sands and gravels of unit B; ii) laminated sand and silt of unit C overlain by the bedded sand and diamicton of unit G; and iii) the uppermost Holocene sequence of littoral gravel with erosional lower contacts (unit H).

The most prominent structure is an asymmetrical ridge-like feature at around 3550 m (Fig. 10A, B). This feature comprises a series of folded and thrusted sediments including a large-scale (amplitude at least 30 m and wavelength ~15m), southwest verging, overturned, tight anticlinal fold affecting the silty-sandy diamicton of unit A and stratified sand and gravel of unit B. This fold overlies a smaller, overturned anticline consisting entirely of unit A. The ridge is deformed by a large number of faults that cut through the sediments on both sides of this feature. These faults are generally curved with a displacement ranging from a few cm to several dm. Most of the faults cutting through the lower limb of the large anticline are normal faults dipping either to the southeast or the northeast whereas both reverse and normal faults are prominent in the upper parts.

The convex upper surface of the ridge is capped by an up to 20 m thick unit of diamictons and stratified sand and gravel of unit B. Internally these gravel and sand beds are undulating and often folded and boudinaged (e.g. at around 3600 m). These beds and the diamicton of unit A can be followed to about 3800 m in the cliff where they have an apparent northward dip with slightly convex upward configuration (Fig. 2). These beds are internally deformed by a number of small faults, mainly normal faults. A number of measurements on faults planes in the lowermost unit (unit A) showed that the faults dip both to the northwest or the southeast (Fig. 10A). An approximately 0.5 m thick layer of deformed (ductile) sediment mélange of folded and layered silt, sand and gravel, which appears to be mostly originated from unit B, separates the stratified sand and gravel from the undeformed laminated silt and sand of unit G above.

Ás-north – structural evolution. The Ás-north zone is, similar to the Belgsholt, Melaleiti and Ásgil zones, mainly characterized by compressive deformation as a result of pressure from a glacier advancing from the north (northeast-northwest) based on the southwest-verging anticlinal folds and the overall northward dip of the thrusted sediment blocks (Fig. 11; e.g. Bennett 2001; Benediktsson *et al.* 2008; Pedersen 2014). The large anticline can be interpreted as recording ductile folding as the ice pushed into the sequence (Fig. 11). Continued ice-push stacked up the sediments above it and in front (south) of this fold, and led to the overturning of this anticline. Thrust faults developed in the upper limb and extensional faults in the lower limb of the anticline formed in response to the overturning and subsequent extension of the fold (Fig. 11).

Comparably to Ásgil, the advance was accompanied an ice-marginal deposition of sands and gravels of unit B, which were subsequently deformed (faulted and boudinaged) possibly in response to continued ice sheet advance. Together with the overturning of the fold this indicates that the moraine underwent subglacial modification (Fig. 11; Aber et al. 1989; Pedersen 2000; van der Wateren 2000; McCarroll & Rijsdijk 2003). However, some of the small normal faults within the gravel (unit B) might have formed by gravity collapse. The sediment mélange capping unit B can be interpreted as a glaciotectonite formed by subglacial shearing of the pre-existing sediments (Evans *et al.* 2006; Benn & Evans, 2010; Ó Cofaigh *et al.* 2011). Alternatively, the mélange can be interpreted as a gravity flow deposited as the ice retreated from the moraine.

Ás-south - structural architecture. Ás-south is the southernmost part of the Ás structural zone (4500-5000 m; Fig. 2, 12). The section wall is 12-20 m high, steeply inclined and oriented NW-SE. Most of the section was visible and easily accessible, which enabled detailed mapping and measurements of sediments and structures.

Ás-south can be divided into three main structural units: i) the folded and faulted zone comprising the stratified sand and gravel of unit B and stratified silty-sandy diamicton of unit A; ii) a deformed silts and sands of unit D with erosive lower contacts which overlies the northern end of unit 1; and iii) the uppermost Holocene sequence of littoral gravels (unit H).

This section comprises a folded and thrusted sequence composed of unit A and B that is cross-cut by open fractures and numerous faults with sharp fault planes. The folds usually become smaller in amplitude towards south. Between ~4800 and 4950 m (Fig. 12A) they are overlain by an indistinctively bedded, silts and sands of unit D, which exhibits ductile deformation structures such as boudins and augen structures. The faults found in the lower units (A and B) usually do not extend upwards into unit D indicating that the faulting predates the deposition of unit D.

Most of the faults form a conjugate set of SE-NW dipping normal faults. The displacement along the planes is commonly in the range of a few cm to a few dm although some have an offset over a meter. This fault pattern is most conspicuous between 4500-4650 m (Fig. 12A) where the faults cross-cut a large, anticlinal open fold with an approximately N-S trending fold axis (Fig. 12A, B), and also in the southernmost part of the cliff between 4800-5000 m (Fig. 12A, C).

In the middle part of the section (4650-4850 m; Fig. 12A), the sequence exhibits a more complex deformation history. Units A and B are folded, thrust repeated and dissected by a number of normal (extensional) and reverse (compressional) faults. These faults cut the sequence at various angles: the normal faults mostly dip to the NW or the SE but thrust faults mainly have a SE dip (Fig. 12A). The fault offsets range from several cm to a few m. A few open fractures infilled by diamicton cut through units A and B in this part of the section. The complicated nature of the deformation in this area made it very hard to trace laterally the individual structural units especially between 4750 and 4800 m (Fig. 12A) where the deformation was most intense.

Ás-south – structural evolution. The large folds indicate that the sequence experienced shortening due to subhorizontal compression consistent with deformation in an ice-marginal or proglacial setting (e.g. Boulton *et al*. 1999; Benediktsson *et al*. 2010). The orientations of the large anticline between 4500-4650 m and the small syncline at around 4980 m (Fig. 12A) could indicate glaciotectonic stress from either the northwest or southeast. The same applies to the system of the conjugate normal faults. The sense of offset along the thrust faults in the central part of the section (~4700-4750 m; Fig. 12A) that cross-cut unit A and B, indicates that these units were affected by a northwestwards directed stress. This is in contrast with all other evidence from the cliffs indicating ice flow from the north. However, these thrust faults are small, they are only seen in a restricted part of the section and the cliff section probably only reveals part of the glaciotectonic zone due to the erosive base of units G and H; hence, they could simply be backthrusts formed in response to localized stress (Boulton *et al.* 1999; Benediktsson *et al.* 2010). Many of the faults and fractures, which cross-cut the folds, were open and infilled by typically massive, coarse sediment indicating extension and subsequent infilling of these fractures. The geometry of the conjugate fault system implies that it was formed by ice-push in association with the folding (Fig. 12A).

There are no unequivocal structural or sedimentological evidence that can tell if the deformation of the sequence was induced by stress from the northwest or southeast. However, as this zone appears to be linked to the tectonic zone at Ás-north (see Fig. 2), pressure from the northwest seems most plausible. In addition, the decreasing amplitude of the folds towards the southeast suggests a decreasing stress in that direction and corresponds to multi-crested end moraine complexes described from modern (e.g. Boulton *et al.* 1999; Benediktsson *et al.* 2010) and Late Weichselian (Phillips *et al*. 2017) glacier environments. This zone is therefore interpreted to represent proglacial folding and faulting of the sediment package in front (south) of the Ás-north thrust zone (Fig. 11).

Discussion

The overall configuration and the internal architecture of the structural zones in the coastal cliffs in Melasveit indicate a series of subaquatic moraines formed during the interplay between glaciotectonic deformation and ice-marginal sedimentation. After the glacier retreated from the area these moraines were covered by glaciomarine, marine and littoral sediments; consequently, the ridges have no or very little topographical expression on the modern land surface. Below we propose a model for the formation of the structural zones/moraines seen in the coastal cliffs in Melasveit and discuss their implications for the regional ice dynamics and glaciotectonic processes below marine-terminating glaciers (Fig. 13, 14).

Direction of ice flow

Directional elements measured in this study, such as large-scale faults, thrusts, fold axes and fold vergence indicate that the glaciotectonic stress was applied from the northwest and north/northeast. Thus, the glacier responsible for the glaciotectonics most likely advanced from Borgarfjörður, which agrees with previous research on the glacial geology and glacial history of this area (Fig. 1A) (e.g. Ingólfsson 1987, 1988; Hart 1994; Ingólfsson & Norðdahl 2001; Norðdahl & Pétursson 2005; Norðdahl *et al.* 2008; Ingólfsson *et al.* 2010; Norðdahl & Ingólfsson 2015). Based on the predominant southeast-ward sense of shearing the lobate-shaped glacier might have been locally flowing from the fjord (Fig. 14).

Hart (1994) and Hart & Roberts (1994) proposed that the deformation in the southernmost part of Melabakkar-Ásbakkar (~4400-5000 m; Fig. 2) was caused by a glacier moving from the south. Although our study revealed a few southward dipping thrust faults at Ás-south (Fig. 12A; ~4700-4750 m), which could support Hart's hypothesis, these were only found at one location and are small-scale compared to the overall deformation observed in the Melabakkar-Ásbakkar cliffs. Also, Ás–south is structurally connected to Ás-north where the glaciotectonic stress direction is most definitely from the north/northwest. Therefore, we suggest that the entire deformation was induced by a glacier flowing southwards from Borgarfjörður.

803 *The formation of the Belgsholt and Melabakkar-Ásbakkar structural zones – a sequential*
804 *model*

805 The internal architecture of the structural zones/moraines is dominated by thrusting and stacking
806 of detached thrust blocks with varying degrees of folding, ductile shearing and brittle faulting
807 (extensional and compressional). Thus, each zone/moraine was formed in the compressional
808 regime of the glacier in an ice-marginal and/or proglacial position and are thus interpreted as
809 moraines formed during advances or still-stands during an overall stepwise northward retreat (e.g.
810 Bennett *et al.* 1999; Bennett 2001; Boulton *et al.* 1999; Phillips *et al.* 2002, 2008, 2017;
811 Benediktsson *et al.* 2010; Benn & Evans 2010; Johnson *et al.* 2013). The moraines are thought to
812 reflect periods where the glacier was grounded transmitting shear stress into the sediments.
813 Between the moraines are zones with no or negligible evidence of glaciotectonic deformation
814 possibly reflecting periods of retreat and lifting of the glacier from the sea bed.

815 The southernmost and largest moraine at Melabakkar-Ásbakkar, the Ás moraine (Ás-north and
816 Ás-south combined) is thought to represent the maximum extent of the glacier. The location of the
817 Ás thrust moraine, the southeast directed sense of ice-push derived from the glaciotectonic
818 structures, and its subtle morphological expression suggest that this moraine system represents a
819 lateral extension of the Skorholtsmelar end-moraine complex further inland (see Fig. 1A), as
820 suggested by Ingólfsson (1988). However, the lack of exposures and obvious morphological
821 expressions of the moraine in the area between the coast and the Skorholtsmelar moraine means
822 that this correlation remains tentative. A sequential glaciotectonic model is proposed for the
823 formation of the moraines/structural zones at Melabakkar-Ásbakkar and Belgsholt associated with
824 the active retreat of a glacier back to Borgarfjörður (Fig. 13, 14). The model is described in twelve
825 separate stages below:

1. The first stage commenced with the advance of the glacier out of Borgarfjörður into the bay (Fig. 1A). Once out of the fjord, the ice spread laterally, extending southward to its proposed maximum limit in the Ás area where it deformed marine sediments of Bølling age (unit A) (Ingólfsson 1988; Ingólfsson *et al.* 2010) to form a prominent, multi-crested thrust moraine (~3500-5000 m; Fig 2). The penecontemporaneous deposition of the ice-marginal sediments of unit B occurred during this advance with the earlier deposited parts of this sequence also being deformed as the glacier continued to advance. The structural architecture of the ice-proximal part of the moraine (Ás-north) is dominated by thrust stacks and overturned folds whereas the ice-distal part of the moraine (Ás-south) comprises open folding of the marine and ice-marginal sediments (units A and B), which are also cross cut by both extensional and compressional faults. These folds observed at Ás-south are thought to have formed at, or some distance in front (proglacial) of the advancing ice margin as a result of the propagation of stress into the forefield.
2. The glacier retreated northwards to an unknown position north of Ás and the laminated silts and sands of unit C were deposited.
3. The glacier re-advanced resulting in an erosion and deformation of the uppermost part of unit C (seen in Ásbakkar between ~3100-3300 m (Fig. 2)). There is no constructional landform visible in the cliff section at this place but only an erosive contact with mainly ductile deformation below. Therefore this remains uncertain.
4. The glacier retreated and the silts and sands of unit D were deposited.
5. The stage 4 retreat was followed by another re-advance causing a thrust stacking at the ice-margin and the formation of a moraine at Ásgil-south (~2600 m; Fig. 2, 8A). This advance was accompanied by a deposition of the ice-marginal outwash sediments of unit B at Ásgil

(Fig. 8A, B) that were subsequently deformed by the ice-push. The subaqueous fan was deposited at the ice margin when the glacier had reached a still-stand position (between 2600-2800 m; Fig. 2, 3B). This fan is undeformed indicating that it was not overridden after it had been deposited. The depression between the ice margin (at Ásgil-south) and the deformation zone at Ásbakkar was gradually infilled by the bedded sediments of unit G.

6. The glacier retreated further north and the silts and sands of unit D found north of Ásgil were deposited.
7. Re-advances or oscillations of the ice margin resulted in ice marginal thrusting and folding of Units A, B and D, and the development of the recessional thrust moraines at Fúla around 600-900 m and possibly other smaller ridges in Fúla Bay.
8. The glacier retreated to the north of the Melabakkar-Ásbakkar coastal cliffs and deposited the interbedded silts and sands of unit E exposed at Melaleiti.
9. The glacier re-advanced causing the thrust stacking and brittle faulting of lithofacies A and E observed at Melaleiti at around 0-300 m (Fig. 2).
10. The glacier advanced to a position somewhere around 2000 m, overriding the thrust-block moraine at Melaleiti and the recessional thrust moraines at Fúla Bay (0-2000 m; Fig. 2). This resulted in a subglacial, extensional deformation, erosion and deposition of subglacial gravels and boulders of unit F on-lapping the thrust-block moraine at Melaleiti and the moraines at Fúla Bay. A moraine composed of imbricated thrust stacked blocks and a subaquatic fan of unit B (between 1500-2000 m; Fig. 2) was formed at the ice margin at Ásgil-north. The folds seen at Ásgil-north (~2250-2400; Fig. 2) most likely represent proglacial folding of the distal (southern) side of the moraine fan. Alternatively, these folds could have been formed due to slumping on the unstable slopes of the moraines at Ásgil or Fúla.

11. The glacier retreated and the depressions between the moraines were rapidly infilled by the upward fining sequence of the bedded marine sediments of unit G (Fig. 2). The lithofacies of unit G are undeformed and overlap the recessional moraines in the Fúla Bay and the thrust-block moraine at Melaleiti with little or no discernible lateral variation in grain size. This indicates concurrent sediment deposition and rapid glacier retreat from Ásgil-north without the formation of ice marginal fans or deformation of the bedded glaciomarine sedimentary infill between the ridges. The glacier retreated to some place north of the study area and the upward fining sequence of unit E exposed at Belgsholt was deposited.
12. This stage occurred following a further phase of retreat and is characterized by the ice-marginal to proglacial folding and thrusting observed at Belgsholt, which is the northernmost and youngest structural zone/-moraine exposed in the coastal cliffs of Melasveit.

Timing of the glacier advances

The exact age of the glacial advances in Melasveit is unknown. Ten radiocarbon dates have been published from the deformed sediments (Units A and D) within the Melaleiti, Ásgil and Ás structural zones ranging between *c*. 13.4 and 14.6 cal. ka BP (Ingólfsson 1987, 1988; Ingólfsson *et al.* 2010; Norðdahl & Ingólfsson 2015). These dates only record the maximum ages of deformation events. Due to lack of *in situ* fossils within the undeformed sediments separating the ridges it has not been possible to determine the minimum age for these events. Ingólfsson (1988) suggested two separate advances based on radiocarbon dates and the stratigraphy of the cliff sections; the first occurring in late Bølling or Allerød (just after *c*. 14.0 cal. ka BP) and the second during the Younger Dryas. However, our model involves a highly dynamic glacier which advanced and retreated multiple times, possibly during a single overall phase of retreat. Our data also indicate that the glaciomarine sediments rapidly accumulated in front of the oscillating glacier continuously providing material for the construction of new moraines. Although it is hard to estimate how rapid this deposition was, studies have shown that deposition rates of ice-proximal sediments similar to the bedded glaciomarine sediments within and between the Melasveit ridges, can be in the order of decimetre or even meters per year (Eyles *et al.* 1985; Cowan *et al.* 1999; Jaeger & Nittrouger 1999; Gilbert *et al.* 2002; Trusel *et al.* 2010).

Based on our model and the age of the sediments in the Melabakkar-Ásbakkar cliffs (Ingólfsson 1988; Ingólfsson *et al.* 2010), the formation of all the moraines may have occurred after *c*. 13.4 cal. ka BP, or most likely during the Younger Dryas chronozone (*c*. 12.8 – 11.7 cal. ka BP). During that time, glaciers in Iceland are known to have expanded considerably and the regional relative sea level was high enough to allow the deposition of the up to 30 m thick marine sediments between and stratigraphically on top of the deformed moraine ridges (Norðdahl *et al.* 2008; Ingólfsson *et al.* 2010).

Conclusions

We have constructed a model of an active retreat of a Late Weichselian, marine-terminating glacier based on a detailed mapping of stratigraphy and glaciotectonics exposed in the coastal cliffs of Belgsholt and Melabakkar-Ásbakkar in Melasveit, lower Borgarfjörður.

- The glaciotectonics reveal a series of well-preserved moraines formed by a marine-terminating glacier advancing from the Borgarfjörður fjord, north of the study area.
- Each moraine marks a former ice-marginal position. Their internal structures are dominated by large-scale thrusting and stacking of detached blocks of marine sediments with varying

degrees of folding, ductile shearing and brittle faulting. This deformation was accompanied by the deposition of ice-marginal subaquatic fans that were largely deformed by continued ice-push and integrated into the glaciotectonics.

- The southernmost and largest structural zone exposed in the Melabakkar-Ásbakkar coastal cliffs is a multi-crested terminal moraine indicating the maximum extent of the Borgarfjörður glacier. The other moraines in the series generally become younger towards the north representing oscillatory advances during an overall northward retreat.
- During this active retreat, glaciomarine sediments were continuously deposited in front of the glacier as source material for new moraines. As the glacier receded, the depressions between the ridges were rapidly infilled by glaciomarine sediments and later, after the isostatic rebound of the area, covered by littoral and aeolian sediments.
- Although the exact age of the glacial advances in Melasveit is unknown, previously obtained radiocarbon ages of marine shells within the deformed marine sediments suggest that these advances most likely occurred during the Younger Dryas chronozone.
- This case study exemplifies glaciotectonic and depositional processes occurring in ice-marginal/proglacial marine environments. It highlights the dynamic nature of marine-terminating glaciers and may aid in the understanding and interpretation of their sedimentological and geomorphological records.

Acknowledgements.This project is funded by the Icelandic Research Fund (grant no. 141002-051 to Í.Ö. Benediktsson), the Royal Physiographic Society in Lund (grants to Th. Sigfúsdóttir and Í.Ö. Benediktsson), with support from the British Geological Survey (to E. Phillips, M. Kirkham, E. Haslam). The LiDAR scanning and photographing of the Melabakkar-Ásbakkar coastal cliffs by Matthew Kirkham and Ed Haslam is gratefully acknowledged. We would like to thank Sandrine Roy,

943 Heimir Ingimarsson and Kim Teilmann for their invaluable assistance and discussions in the field,
944 and Ólafur Ingólfsson and Hreggviður Norðdahl for fruitful discussions on the glacial history of the
945 area. Furthermore, we also thank Per Möller for his useful comments on the manuscript and James
946 Aber and Matthew Bennett for constructive reviews that helped us improve this paper. E. Phillips
947 publishes with the permission of the Executive Director of the British Geological Survey, NERC.

948 **References**

949 Aber, J. S. & Ber, A. 2007: *Glaciotectonism*. 256 pp. *Developments in Quaternary Science 6*. Elsevier,
950 Amsterdam.

951 Aber, J. S., Croot, D. G. & Fenton, M. M. 1989: *Glaciotectonic landforms and structures*. 200 pp.
952 *Glaciology and Quaternary Geology Series*. Kluwer Academic Publishers, Dordrecht.

953 Allmendinger, R. W., Cardozo, N. C. & Fisher, D. M. 2012: *Structural Geology Algorithms: Vectors*
954 *and Tensors*. 302 pp. Cambridge University Press, Cambridge.

955 Benediktsson, Í. Ö., Möller, P., Ingólfsson, Ó., van der Meer, J. J. M., Kjær, K. H. & Krüger, K. 2008:
956 Instantaneous end moraine and sediment wedge formation during the 1890 surge of Brúarjökull,
957 Iceland. *Quaternary Science Reviews 27*, 209-234.

958 Benediktsson, Í. Ö., Schomacker, A., Lokrantz, H. & Ingólfsson, Ó. 2010: The 1890 surge end
959 moraine at Eyjabakkajökull, Iceland: a re-assessment of a classic glaciotectonic locality. *Quaternary*
960 *Science Reviews 29*, 484-506.

961 Benediktsson, Í. Ö., Schomacker, A., Johnson, M. D., Geiger, A.J., Ingólfsson, Ó. & Guðmundsdóttir,
962 E. R. 2015: Architecture and structural evolution of an early Little Ice Age terminal moraine at the
963 surge-type glacier Múlajökull, Iceland. *Journal of Geophysical Research 120*, 1895-1910.

Benn, D. I. & Evans, D. J. A. 2010: *Glaciers and Glaciation*. 802 pp. Hodder education, London.

Bennett, M. R. 2001. The morphology, structural evolution and significance of push moraines. *Earth-Science Reviews 53*, 197-236.

Bennett, M. R., Hambrey, M. J., Huddart, D., Glasser, N. F. & Crawford, K. 1999: The landform and sediment assemblage produced by a tidewater glacier surge in Kongsfjorden, Svalbard. *Quaternary Science Reviews 18*, 1213-1246.

Bennett, M. R., Huddart, D., Waller, R. I., Cassidy, N., Tomio, A., Zukowskyj, P., Midgley, N. G., Cook, S. J., Gonzalez, S. & Glasser, N. F. 2004: Sedimentary and tectonic architecture of a large push moraine: a case study from Hagafellsjökull - Eystri, Iceland. *Sedimentary Geology 172*, 269-292.

Boggs, S. 2006: *Principles of Sedimentology and Stratigraphy*. 662 pp. Pearson Prentice Hall, Upper Saddle River.

Boulton, G. S., van der Meer, J. J. M., Beets, D. J., Hart., J. K. & Ruegg, G. H. J. 1999: The sedimentary and structural evolution of a recent push moraine complex: Holmstrømbreen, Spitsbergen. *Quaternary Science Reviews 18*, 339-371.

Boulton, G. S., van der Meer, J. J. M., Hart, J, Beets, D., Ruegg, G. H. J., van der Wateren, F. M. & Jarvis, J. 1996: Till and moraine emplacement in a deforming bed surge - an example from a marine environment. *Quaternary Science Reviews 15*, 691-987.

Cardozo, N. & Allmendinger, R. W. 2013: Spherical projections with OSXStereonet. *Computers and Geosciences* 51, 193-205.

Clark, P. U., Dyke, A. S., Shakun, J. D., Carlson, A. E., Wohlfarth, B., Mitrovica, J. X., Hostetler, S. W. & McCabe, A. M. 2009: The last glacial maximum. *Science 325*, 710-714.

Cowan, E. A, Seramur, K. C., Cai, J. & Powell., R. D. 1999: Cyclic sedimentation produced by fluctuations in meltwater discharge, tides and marine productivity in an Alaskan fjord. *Sedimentology 46*, 1109-1126.

Croot, D. G. 1987: Glacio-tectonic structures: a mesoscale model of thin-skinned thrust sheets? *Journal of Structural Geology 9,* 797-808.

Dowdeswell, J. A. & Vásquez, M. 2013: Submarine landforms in the fjords of southern Chile: implications for glacimarine processes and sedimentation in a mild glacier-influenced environment. *Quaternary Science Reviews 64*, 1-19.

Dyke, A. S., Andrews, J. T., Clark, P. U., England, J. H., Miller, G. H., Shaw, J. & Veillette, J. J. 2002: The Laurentide and Innuitian ice sheets during the Last Glacial Maximum. *Quaternary Science Reviews 21*, 9-31.

Evans, D. J. A. & Benn, D. I. 2004: *A Practical Guide to the Study of Glacial Sediments*. 266 pp. Arnold, London.

Evans, D. J. A., Phillips, E. R, Hiemstra, J. F. & Auton, C. A. 2006: Subglacial till: Formation, sedimentary characteristics and classification. *Earth-Science Reviews 78*, 115-176.

Flink, A. E., Noormets, R., Kirchner, N., Benn, D. I., Luckman, A. & Lovell., H. 2015: The evolution of a submarine landform record following recent and multiple surges of Tunabreen glacier, Svalbard. *Quaternary Science Reviews 108*, 37-50.

Franzson, H. 1978: *Structures and petrochemistry of the Hafnarfjall-Skarðsheiði central volcano and the surrounding basalt succession, W-Iceland*. Ph.D. thesis, University of Edinburgh, 264 pp.

Gilbert, R., Nielsen, N., Möller, H., Desloges, J.R. & Rasch, M. 2002: Glacimarine sedimentation in Kangerdluk (Disko Fjord), West Greenland, in response to a surging glacier. *Marine Geology 191*, 1-18.

Harris, C., Williams, G., Brabham, P., Eaton, G. & McCarroll, D. 1997: Glaciotectonized Quaternary sediments at Dinas Dinlle, Gwynedd, North Wales, and their bearing on the style of deglaciation in the Eastern Irish Sea. *Quaternary Science Reviews 16*, 109-127.

Hart, J. K. 1994: Proglacial glaciotectonic deformation at Melabakkar- Asbakkar, west Iceland. *Boreas 23*, 112-121.

Hart, J. K. & Roberts, D. H. 1994: Criteria to distinguish between subglacial glaciotectonic and glaciomarine sedimentation, I. Deformation styles and sedimentology. *Sedimentary Geology 91*, 191-213.

Hughes, A. L. C., Gyllencreutz, R., Lohne, Ø. S., Mangerud, J. & Svendsen, J. I. 2016: The last Eurasian ice sheets – a chronological database and time-slice reconstruction, DATED-1. *Boreas,* 45, 1-45.

Håkansson, S. 1983: A reservoir age for the coastal waters of Iceland. *GFF 105*, 65–68.

Ingólfsson, Ó. 1987: The Late Weichselian glacial geology of the Melabakkar- Ásbakkar coastal cliffs, Borgarfjörður, W-Iceland. *Jökull 37*, 57-81.

Ingólfsson, Ó. 1988: Glacial history of the lower Borgarfjörður area, western Iceland. *GFF 110*, 293-309.

Ingólfsson, Ó., Norðdahl, H. & Schomacker, A. 2010: Deglaciation and Holocene Glacial History of Iceland. *Developments in Quaternary Sciences 13*, 51-68.

Ingólfsson, Ó. & Norðdahl, H. 2001: High relative sea level during the Bølling interstadial in Western Iceland: a reflection of ice-shelf collapse and extremely rapid glacial unloading. *Arctic, Antarctic, and Alpine Research 33*, 231-243.

Jaeger, J. M. & Nittrouer, C. A. 1999: Marine record of surge-induced outburst floods from the Bering Glacier, Alaska. *Geology 27*, 847-850.

Jennings, A., Syvitski, J., Gerson, L., Grönvold, K., Geirsdóttir, Á., Harðardóttir, J., Andrews, J. & Hagen, S. 2000: Chronology and paleoenvironments during the late Weichselian deglaciation of the southwest Iceland shelf. *Boreas 29*, 167-183.

Johnson, M.D., Benediktsson, Í, Ö. & Björklund, L. 2013: The Ledsjö end moraine – a subaquatic push moraine composed of glaciomarine clay in central Sweden. *Proceedings of the Geologists Association 124*, 738-752.

Johnson, M.D. & Ståhl, Y. 2010: Stratigraphy, sedimentology, age and palaeoenvironment of marine varved clay in the Middle Swedish end-moraine zone. *Boreas 39*, 199-214.

Kjær, K. H., Larsen, E., van der Meer, J. J .M., Ingólfsson, Ó., Krüger, J., Benediktsson, Í. Ö., Knudsen, C. G. & Schomacker, A. 2006: Subglacial decoupling at the sediment/bedrock interface: a new mechanism for rapid flowing ice. *Quaternary Science Reviews 25*, 2704-2712.

Krüger, J. & Kjær, K. H. 1999: A data chart for field description and genetic interpretation of glacial diamicts and associated sediments - with examples from Greenland, Iceland, and Denmark. *Boreas 28*, 386- 402.

Lee, J. R. & Phillips, E. 2013: Glaciotectonics-a key approach to examining ice dynamics, substrate rheology and ice-bed coupling. *Proceedings of the Geologists' Association 124*, 731-737.

Lee, J. R., Phillips, E., Booth, S. J., Rose, J., Jordan, H. M., Pawley, S. M., Warren, M. & Lawley, R. S. 2013: A polyphase glacitectonic model for ice-marginal retreat and terminal moraine development: the Middle Pleistocene British Ice Sheet, northern Norfolk, UK. *Proceedings of the Geologists' Association 124*, 753-777.

Lønne, I. 1995: Sedimentary facies and depositional architecture of ice-contact glaciomarine systems. *Sedimentary Geology 98*, 13-43.

Lønne, I. & Nemec, W. 2011: The kinematics of ancient tidewater ice margins: Criteria for recognition from grounding-line moraines. *Geological Society of London Special Publications 354*, 57-75.

Lønne, I., Nemec, W., Blikra, L.H. & Lauritsen, T. 2001: Sedimentary architecture and dynamic stratigraphy of a marine ice-contact system. *Journal of Sedimentary Research 71*, 922-943.

Magnúsdóttir, M. & Norðdahl, H. 2000: Aldur hvalbeins og fornra fjörumarka í Akrafjalli (English summary: Re-examination of the deglaciation history of the area around Akrafjall in South-western Iceland). *Náttúrufræðingurinn 69*, 177-188.

Maizels, J. 1997: Jökulhlaup deposits in proglacial areas. *Quaternary Science Reviews 16*, 793-819.

Marren, P. M. 2005: Magnitude and frequency in proglacial rivers: a geomorphological and sedimentological perspective. *Earth-Science Reviews 70*, 203-251.

van der Meer, J.J.M., Kjær, K.H., Krüger, J., Rabassa, J. & Kilfeather, A.A. 2009: Under pressure: clastic dykes in glacial settings. *Quaternary Science Reviews 28*, 708-720.

McCarroll, D. & Rijsdijk, K. F. 2003: Deformation styles as a key for interpreting glacial depositional environments. *Journal of Quaternary Science 18*, 473-489.

Nichols, G. 2009: *Sedimentology and Stratigraphy*, 432 pp. Wiley-Blackwell, Oxford.

Norðdahl, H. & Ingólfsson, Ó. 2015: Collapse of the Icelandic ice sheet controlled by sea-level rise? *Arktos 1*, 13.

Norðdahl, H., Ingólfsson, Ó., Pétursson, H. G. & Hallsdóttir, M. 2008: Late Weichselian and Holocene environmental history of Iceland. *Jökull 58*, 343-364.

Norðdahl, H. & Pétursson, H. G. 2005: Relative sea level changes in Iceland: New aspects of the Weichselian deglaciation of Iceland. In: Iceland-Modern Processes and Past Environments. Eds. Caseldine, C., Russel, A., Harðardóttir, J. & Knudsen, Ó. *Developments in Quaternary Science 5*, 25-78.

Ottesen, D. & Dowdeswell, J. A. 2006: Assemblages of submarine landforms produced by tidewater glaciers in Svalbard. *Journal of Geophysical Research 111*, F01016. doi: 10.1029/2005JF000330.

Ottesen, D., Dowdeswell J. A., Benn, D. I., Kristensen, L., Christiansen, H. H., Christensen. O., Hansen, L., Lebesbye, E., Forwick, M. & Vorren, T.O. 2008: Submarine landforms characteristics of glacier surges in two Spitsbergen fjords. *Quaternary Science Reviews 27*, 1583-1599.

Ó Cofaigh, C. & Dowdeswell, J. A. 2001: Laminated sediments in a glacimarine environments: diagnostic criteria for their interpretation. *Quaternary Science Reviews 20*, 1411-1436.

Ó Cofaigh, C., Dunlop, P. & Benetti, S. 2012: Marine geophysical evidence for Late Pleistocene ice sheet extent and recession off northwest Ireland. *Quaternary Science Reviews 44*, 147-159.

Ó Cofaigh, C., Evans, D. J. A. & Hiemstra, J. F. 2011: Formation of a stratified subglacial 'till' assemblage by ice-marginal thrusting and glacier overriding. *Boreas 40*, 1-14.

Patton, H., Hubbard, A., Bradwell, T. & Schomacker, A. 2017: The configuration, sensitivity and rapid retreat of the Late-Weichselian Icelandic ice sheet. *Earth Science Reviews 166*, 223-245.

Pedersen, S.A.S. 2000. Superimposed deformation in glaciotectonics. *Bulletin of Geological Society of Denmark 46*, 125-46.

Pedersen, S. A. S. 2005: Structural analysis of the Rubjerg Knude glaciotectonic complex, Vendsyssel, northern Denmark. *Geological Survey of Denmark and Greenland, Bulletin 8*, 192 pp.

Pedersen, S. A. S. 2014: Architecture of Glaciotectonic Complexes. *Geosciences 4*, 269-296.

Phillips, E. R, Evans, D. J. A. & Auton, C.A. 2002: Polyphase deformation at an oscillating ice margin following the Loch Lomond Readvance, central Scotland, UK. *Sedimentary Geology 149*, 157-182.

Phillips, E., Lee, J. R. & Burke, H. 2008: Progressive proglacial to subglacial deformation and syntectonic sedimentation at the margins of the Mid-Pleistocene British Ice Sheets: evidence from north Norfolk, UK. *Quaternary Science Reviews 27*, 1848-1871.

Phillips, E., Lee, J. R. & Evans, H. M. 2011: *Glacitectonics - Field Guide*. Quaternary Research Association, Pontypool.

Phillips, E. & Merritt, J. 2008: Evidence for multiphase water-escape during rafting of shelly marine sediments at Clava, Inverness-shire, NE Scotland. *Quaternary Science Reviews 27*, 988-1011.

Phillips, E. & Hughes, L. 2014. Hydrofracturing in response to the development of an overpressurised subglacial meltwater system during drumlin formation: an example from Anglesey, NW Wales. *Proceedings of the Geologists’ Association* 125, 269-311.

Phillips, E. 2017: Glacitectonics. *In* Menzies, J. & van der Meer, J. J .M. (eds.): *Past Glacial Environments, 467-502*. Elsevier, Amsterdam, Oxford, Cambridge MA.

Phillips, E., Cotterill, C., Johnson, K., Crombie, K., James, L., Carr, S., Ruiter, A. 2017: Large-scale glaciotectonic deformation in response to active ice sheet retreat across Dogger Bank, (southern central North Sea) during the Last Glacial Maximum. *Quaternary Science Reviews 179*, 24-47.

Powell, R. D. 2003: Subaquatic land systems: fjords. In Evans, D.J.A. (ed.): *Glacial Landsystems*, 313-347. Arnold, London.

Powell, R. D. & Domack, E. W. 1995*:* Modern glaciomarine environment: In Menzies, J. (ed.): Modern Glacial Environments: Processes, Dynamics, and Sediments; Glacial Environments 1, 445-486. Oxford, Butterworth-Heinmann.

Powell, R. D. & Molnia, B. F. 1989: Glacimarine sedimentary processes, lithofacies and morphology of the south-southeast Alaska shelf and fjords. *Marine Geology 85*, 359-390.

Reimer, P. J., Bard, E., Bayliss, A., Beck, J. W., Blackwell, P. G., Bronk, Ramsey, C., Buck, C. E., Cheng, H., Edwards, R. L., Friedrich, M., Grootes, P. M., Guilderson, T. P., Haflidason, H., Hajdas, I., Hatté, C., Heaton, T. J., Hoffmann, D. L., Hogg, A. G., Hughen, K. A., Kaiser, K. F., Kromer, B., Manning, S. W., Niu, M., Reimer, R. W., Richards, D. A., Scott, E. M., Southon, J. R., Staff, R. A., Turney, C. S. M. & van der Plicht, J. 2013. IntCal13 and Marine13 Radiocarbon Age Calibration Curves 0-50,000 Years cal BP. *Radiocarbon 55*, 1869-1887.

Rijsdijk, K. F., Warren, W. P. & van der Meer, J. J. M. 2010: The glacial sequence at Killiney, SE Ireland: terrestrial deglaciation and polyphase glacitectonic deformation. *Quaternary Science Reviews 29*, 696-719.

Rijsdijk, K. F., Owen, G., Warren, W. P., McCarroll, D. & van der Meer, J. .J. M. 1999: Clastic dykes in over-consolidated tills: evidence for subglacial hydrofracturing at Killiney Bay, eastern Ireland. *Sedimentary Geology 129*, 111-126.

Russell, A. J., Roberts, M. J., Fay, H., Marren, P. M., Cassidy, N. J., Tweed, F. S. & Harris, T. 2006: Icelandic jökulhlaup impacts: implications for ice-sheet hydrology, sediment transfer and geomorphology. *Geomorphology 75*, 33-64.

Rydningen, T. A., Vorren, T. O., Laberg, J. S. & Kolstad, V, 2013: The marine-based NW Fennoscandian ice sheet: glacial and deglacial dynamics as reconstructed from submarine landforms. *Quaternary Science Reviews 68*, 126-141.

Seramur, K. C., Powell, R. D. & Carlson, P. R. 1997: Evaluation of conditions along the grounding line of temperate marine glaciers: an example from Muir Inlet, Glacier Bay, Alaska. *Marine Geology 140*, 307-327.

Símonarson, L. 1981: Upper Pleistocene and Holocene marine deposits and faunas on the north coast of Nugssuaq, West Greenland. *Grønlands geologiske undersøgelse 140*, 1-107.

Syvitski, J. P., Jennings, A. E. & Andrews, J. T. 1999: High-resolution seismic evidence for multiple glaciation across the southwest Iceland Shelf. *Arctic, Antarctic, and Alpine Research 31*, 50-57.

Sættem, J. 1994: Glaciotectonic structures along the southern Barents shelf margin. *In* Warren, W.P. & Croot, D.G. (eds.): *Formation and deformation of glacial deposits*, 95-113. A.A. Balkema, Rotterdam.

Thomas, G. S. P. & Chiverrell, R. C. 2007: Structural and depositional evidence for repeated ice-marginal oscillation along the eastern margin of the Late Devensian Irish Sea Ice Stream. *Quaternary Science Reviews 26*, 2375-2405.

Trusel, L. D., Powell, R. D., Cumpston, R. M. & Brigham-Grette, J. 2010: Modern glacimarine processes and potential future behaviour of Kronebreen and Kongsvegen polythermal tidewater glaciers, Kongsfjorden, Svalbard. *The Geological Society of London, Special Publications 344*, 89-102.

Vaughan - Hirsch, D. P., Phillips, E., Lee, J. R. & Hart, J. 2013: Micromorphological analysis of poly-phase deformation associated with the transport and emplacement of glaciotectonic rafts at West Runton, north Norfolk, UK. *Boreas 42*, 376-394.

van der Wateren, F. M., Kluiving, S. J. & Bartek, L. R. 2000: Kinematic indicators of subglacial shearing. *In* Maltman, A. J., Hubbard, B. & Hambrey, M. J. (eds.): *Deformation of Glacial Materials*, 259-278. *Geological Society of London, Special Publications 176*.

Williams, G. D., Brabham, P. J., Eaton, G. P. & Harris, C. 2001: Late Devensian glaciotectonic deformation at St Bees, Cumbria: a critical wedge model. *Journal of the Geological Society 158*, 125-135.

Winkelmann, D., Jokat, W., Jensen, L. & Schenke, H-W. 2010: Submarine end moraines on the continental shelf off NE Greenland- Implications for Late Glacial dynamics. *Quaternary Science Reviews 29*, 1069-1077.

List of Figure captions:

Figure 1. A. The Melasveit study area (red box) and the surrounding regions. Arrows indicate the ice flow into the region during the Weichselian glaciation according to Ingólfsson (1988). B. A map of Melasveit. Thick black lines indicate the Belgsholt and Melabakkar-Ásbakkar coastal sections and blue lines the structural zones which were studied in detail in this paper.

C. The northern part of the Melabakkar coastal cliff. D. The Belgsholt coastal section. Note the ridge-like shape of the landform that contains the section.

Figure 2. Overview diagrams of the coastal cliffs from Belgsholt in the north throughout Melabakkar-Ásbakkar. The diagrams where drawn on the basis of terrestrial LiDAR images, except at ~400-2000 and 3900-4500 m, where photographs were used. The diagram is vertically exaggerated (2x). Shaded areas represent sections covered by water and debris that prevented detailed investigation of both structures and stratigraphy.

Figure 3. Examples of sediment composition and contact configuration within some of the eight (A-H) identified sediment units within the Melabakkar-Ásbakkar coastal cliffs. A. Close-up view of the silty-sandy diamicton of unit A (Melaleiti at ~100 m, Fig. 2). Note the embedded unbroken *Chlamys islandica* shell. B. Unit D silts and sands of overlaying unit B stratified sand and gravel. The contact between the sediment units is sheared and folded and is cross cut by a number of small faults. On top in unit H beach-face sediment. Cliff section at around 2550 m (Fig. 2). C. Unit B locally upward coarsening beds of stratified sand and gravel; the gravel is mostly undeformed and forms a ~15 m thick sediment pile, in turn overlain by undeformed unit G interbedded diamicton and sand. Cliff section at about 2650 m (Fig. 2). D. Unit C horizontally laminated silt and sand grading upwards into a heterogeneous diamicton. The basal sediment sequence is conformably overlain by unit G sandy beds which at this location dip towards north. The unit A silty-sandy diamicton can be seen at beach level. Cliff section at ~3200 m (Fig. 2). E. Unit E interbedded silt and sand at the base of the cliff with unit A diamicton trusted on top. Melaleiti cliff section at ~250 m (Fig.2). F. Unit A silty-sandy diamicton, overlain by a 2 m thick bed of massive gravel and boulders (unit F) with erosive

contact in between. Stratified and undeformed unit G drape the unit F gravel. Cliff section at ~1300-1350 m (Fig. 2).

Figure 4. The structural ridge at Belgsholt. A. A scale diagram of the Belgsholt section above a LiDAR image of the section. Directional data are plotted on lower hemisphere stereographic projections and the blue bars indicate the orientation of the section. The white squares indicate the area covered by photos 4B and C. B. A large syncline at ~70 m. C: An overturned, southward verging anticline at ~90 m. Note the big boulder (1 m in diameter) approximately in the core of the anticline.

Figure 5. A. A scale diagram and a LiDAR image of the Melaleiti structural zone. Directional data are plotted on lower hemisphere stereographic projections and the blue bars indicate the orientation of the section. The white squares indicate the area covered by photos 5B-D. B. Stacked rafts of unit A silty-sandy diamicton separated by deformed unit E interbedded silt and sand. Note the person for scale C. Boudinaged raft of silty-sandy diamicton of unit A with faulted unit E bedded sediments below. D. A close-up view of faults cutting through unit E sediments. Spade for scale.

Figure 6. A sequential model showing the formation of the Melaleiti structural zone.

Figure 7. A photo of the Fúla bay thrust zone at ~730m (Fig. 2). Directional data are plotted on lower hemisphere stereographic projections and the blue bars indicate the orientation of the section.

Figure 8. A. A scale diagram and a LiDAR image of the Ásgil section. Directional data are plotted on lower hemisphere stereographic projections and the blue bars indicate the orientation of the section. The black squares on the Lidar image indicate locations of photos

7B–D. B. Imbricated thrust blocks of unit D at ~2475 m. The lower thrust block is folded and dissected by normal faults with a southwest dip. C. Shear zone separating the silts and sands of unit D above and the stratified sand and gravel of unit B below. D. A hydrofracture dissecting a bed of massive sandy-silt belonging to unit D, infilled with sorted coarse sand from unit B below.

Figure. 9. A sequential model explaining the formation of the southern part of the Ásgil structural zone.

Figure 10. A. A scale diagram and a LiDAR image of the Ás-north section. Directional data are plotted on a lower hemisphere stereographic projection and the blue bars indicate the orientation of the section. The black box indicates the location of photograph 8B. B. A large overturned, southwestward verging and deformed anticlinal fold affecting lithofacies 1 and 4. It is truncated by a number of shear planes with an apparent sense of displacement towards the south and dissected by a number of both extensional and compressional faults.

Figure 11. A sequential model showing the formation of the Ás structural zone (north and south).

Figure 12. A. A scale diagram and a LiDAR image of the Ás-south section. Directional data are plotted on a lower hemisphere stereographic projection and the blue bar indicates the orientation of the section. The white squares indicate the locations of photographs 9B and 9C. B. The northern limb of an open anticlinal fold affecting the stratified diamicton of unit A. The fold is dissected by numerous normal faults. C. Faulted sediments of units A and B overlain by sheared and deformed diamicton of unit D.

Figure 13. A conceptual sequential model demonstrating the formation of the glaciotectonic moraines exposed in the coastal cliffs of Belgsholt and Melabakkar-Ásbakkar. The sequence of events is described in the Discussion section. Black arrows indicate displacement and blue arrows indicate water flow. Brown: pre-existing fossilifereous silty-sandy glaciomarine diamicton (unit A), green: ice-marginal/sub-glacial fluvial sediments (units B and F), yellow: deformed laminated/bedded glaciomarine sediments (units C, D and E), and grey: undeformed, bedded glaciomarine sediments (unit G).

Figure 14. A hillshade map of the study area showing the location of the moraines exposed in the coastal cliffs (red lines) and the configuration of the moraines based on structural data from this study (black solid lines). Note that the configuration of the youngest moraine at Belgsholt was formed by glaciotectonic stress from the north while the stress forming all the older moraines was, at least locally, applied from the northwest. Black dashed lines are an approximation of the configuration of the ice margin during each advance, partly based on the correlation between the Skorholtsmelar moraine and the Ás structural zone. The numbers refer to the relative timing of advances (see Fig. 13).

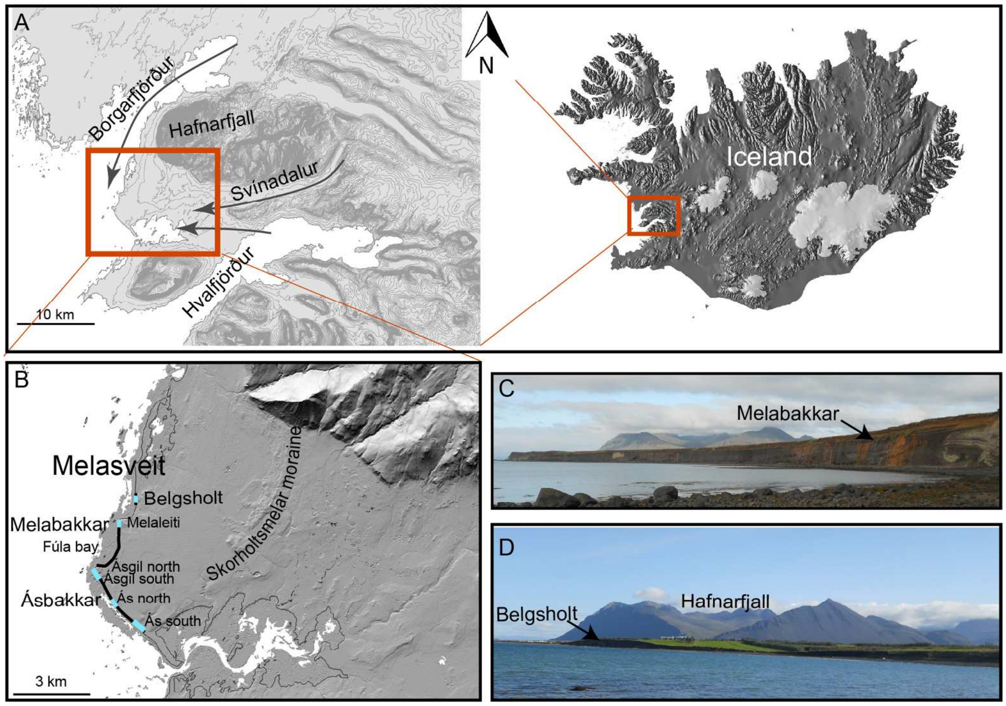

183x128mm (300 x 300 DPI)

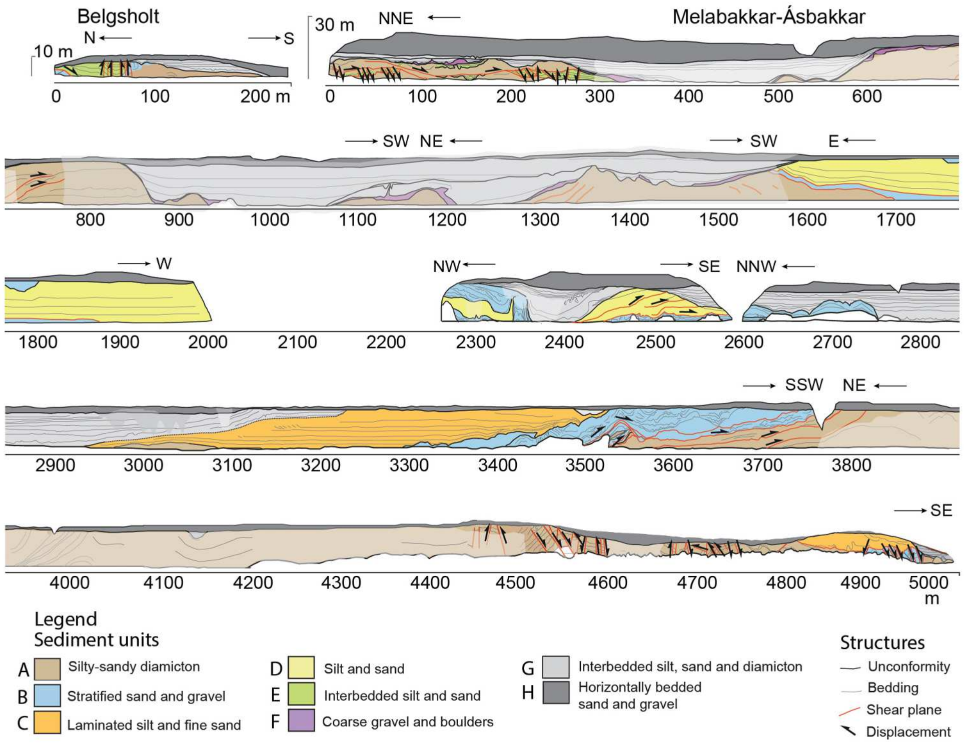

176x147mm (300 x 300 DPI)

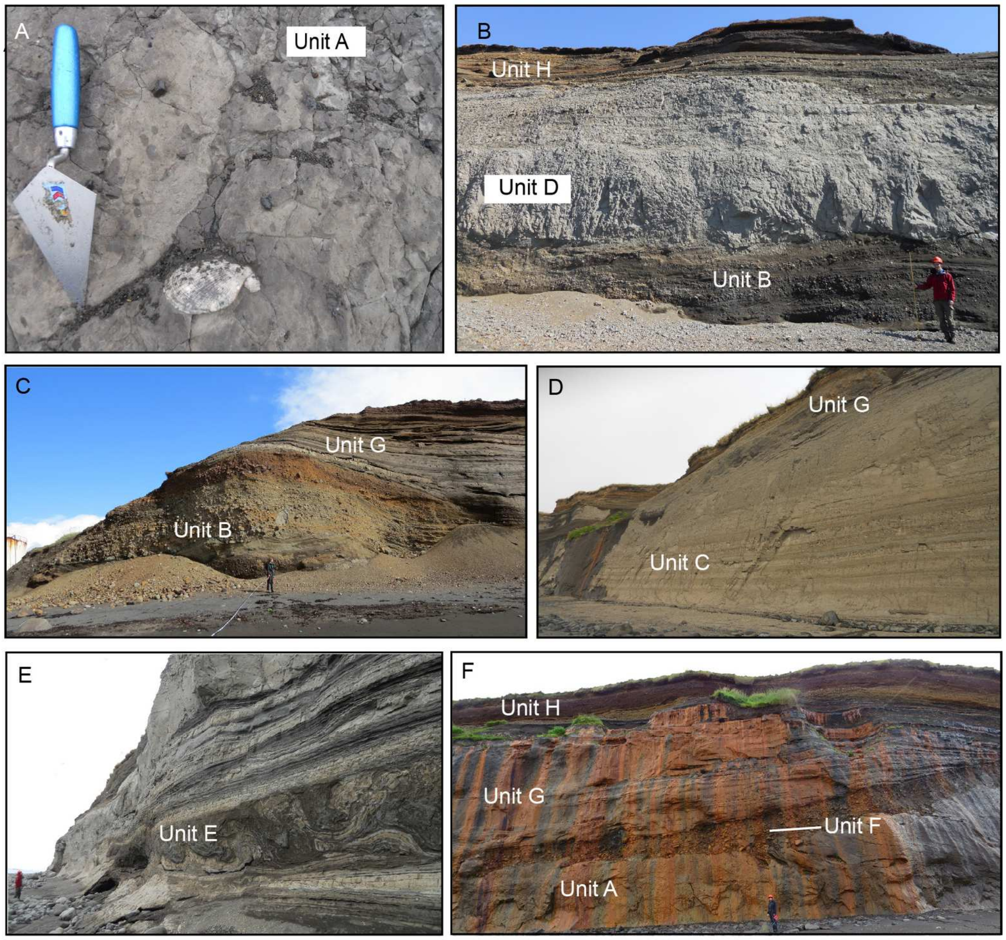

166x157mm (300 x 300 DPI)

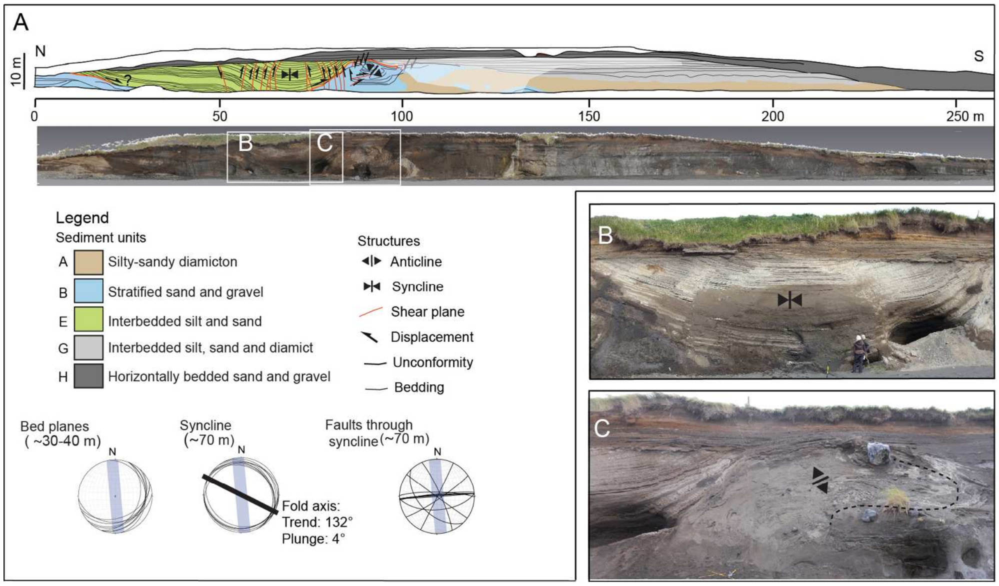

168x100mm (300 x 300 DPI)

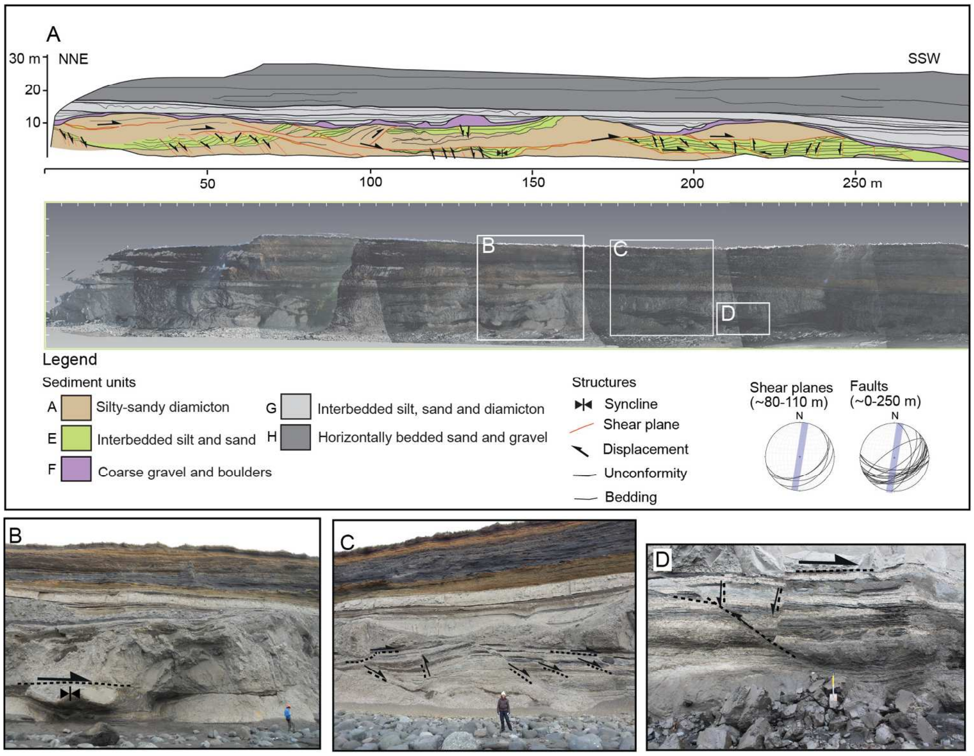

171x133mm (300 x 300 DPI)

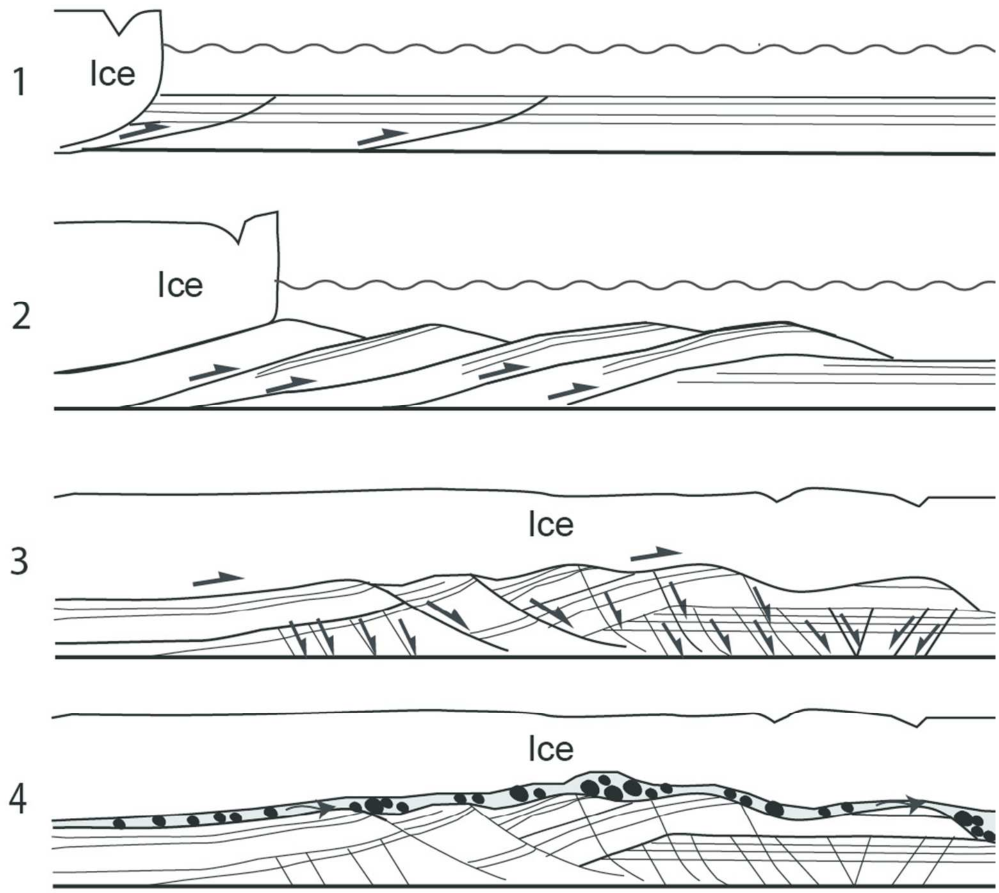

88x82mm (300 x 300 DPI)

95x43mm (300 x 300 DPI)

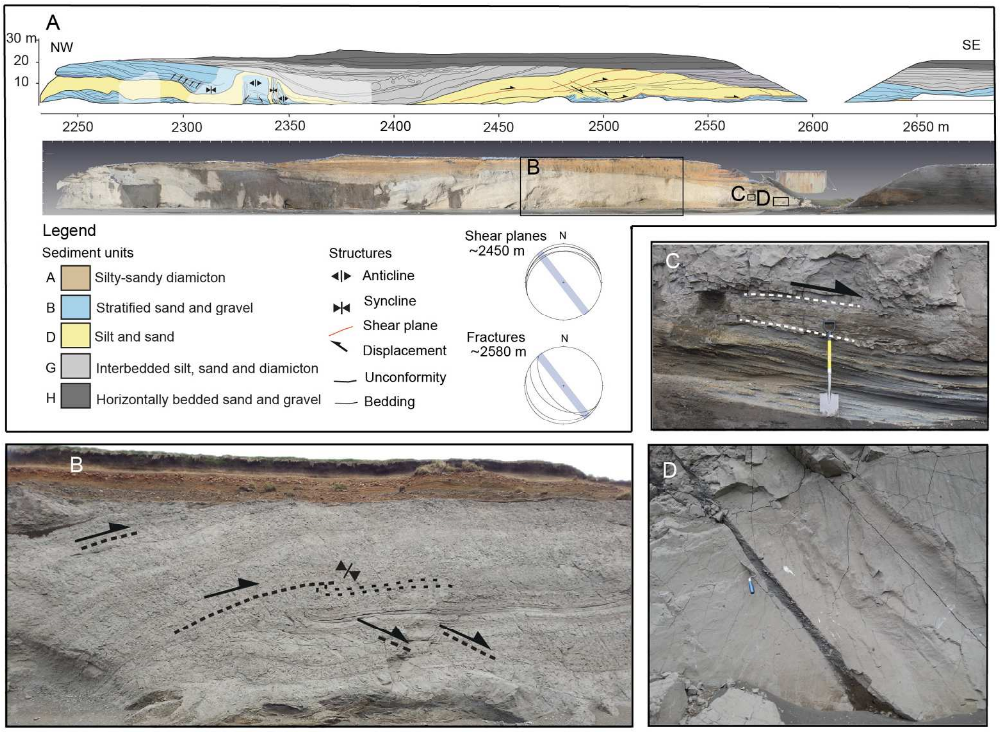

172x126mm (300 x 300 DPI)

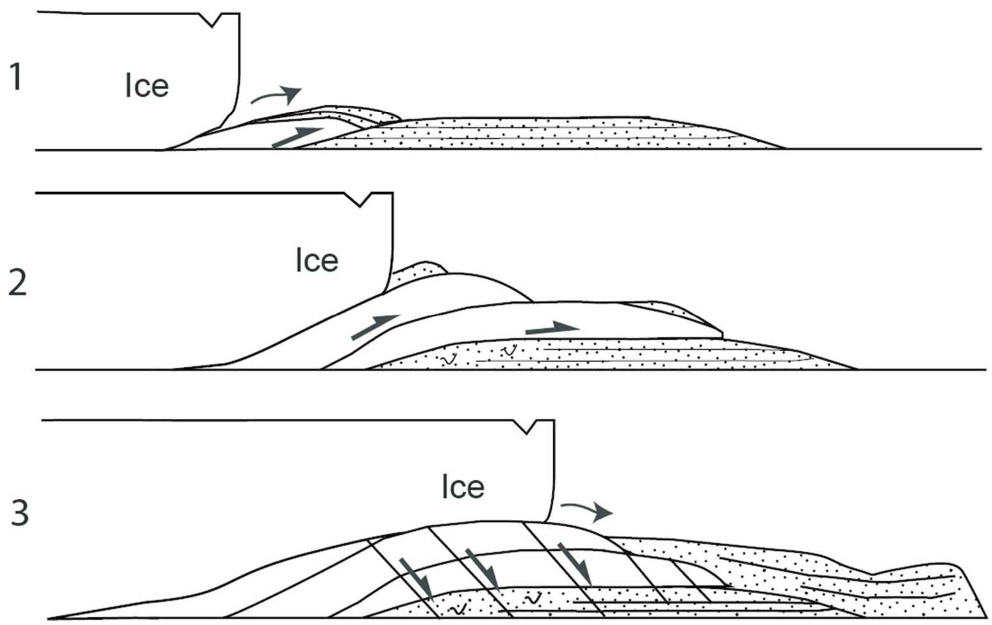

93x57mm (300 x 300 DPI)

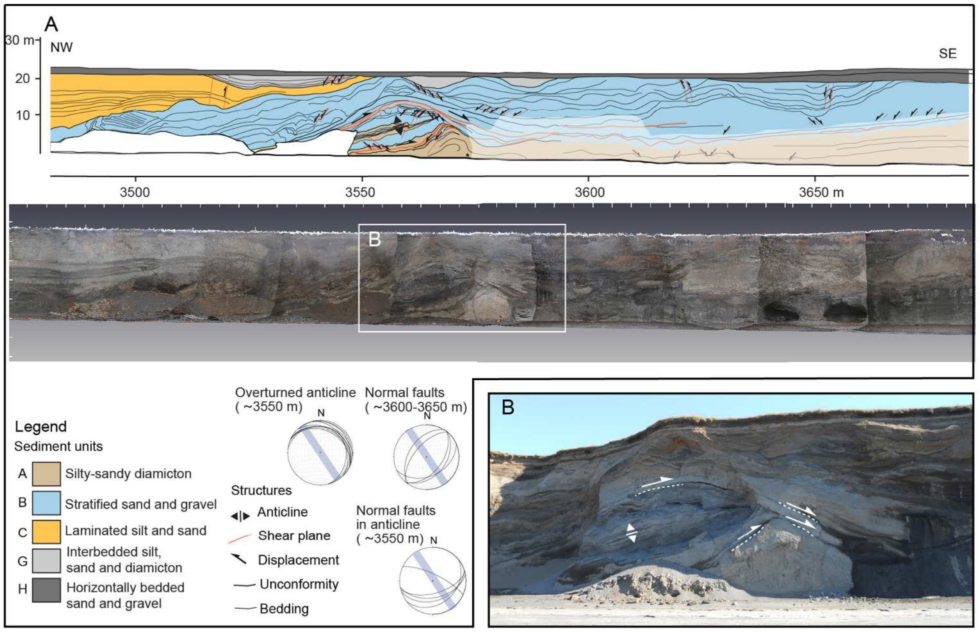

177x112mm (300 x 300 DPI)

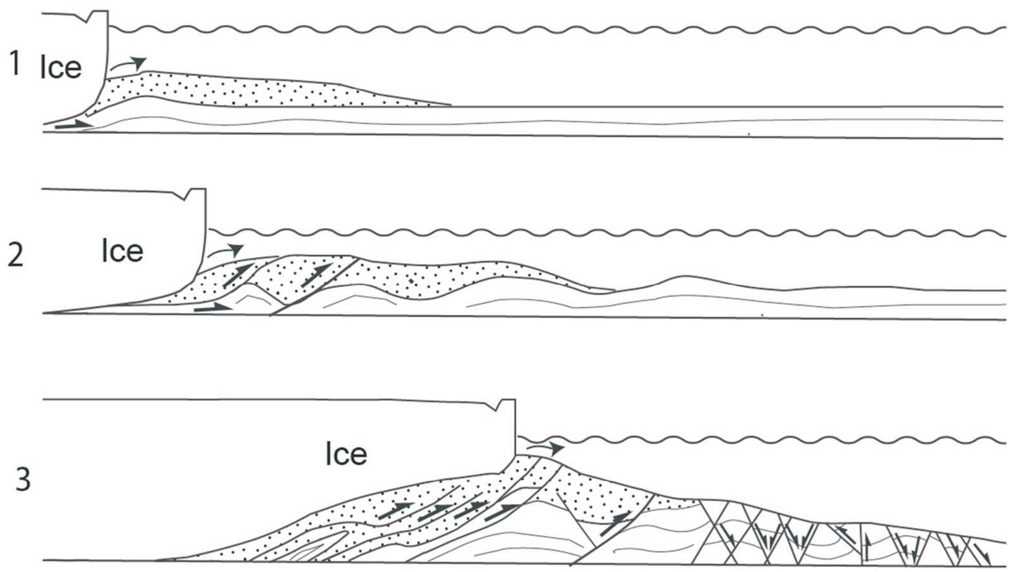

96x56mm (300 x 300 DPI)

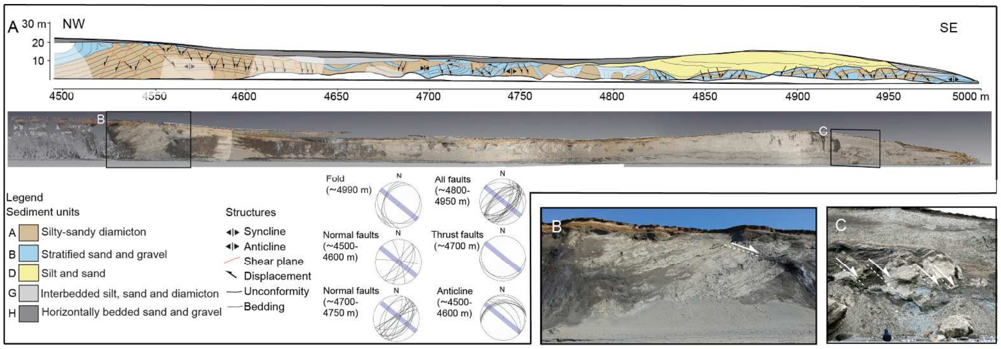

222x77mm (300 x 300 DPI)

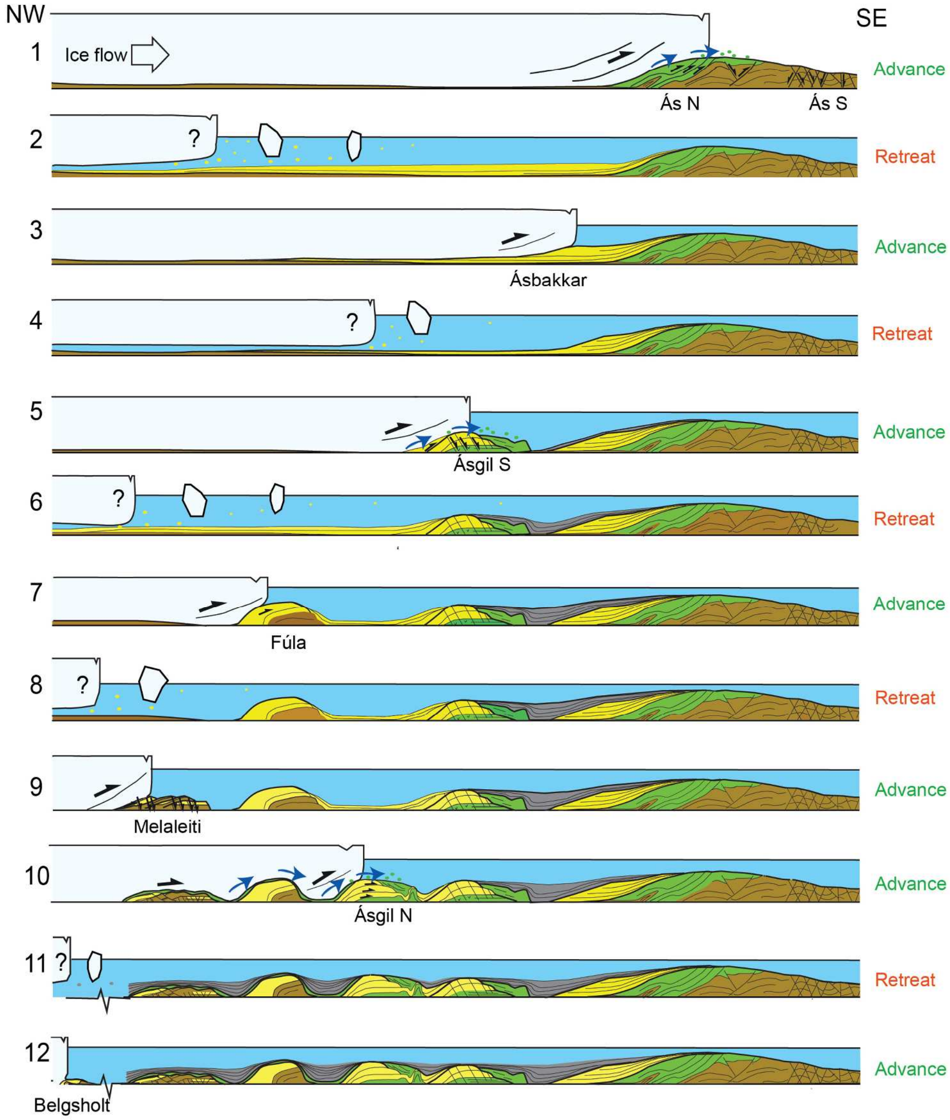

200x236mm (300 x 300 DPI)

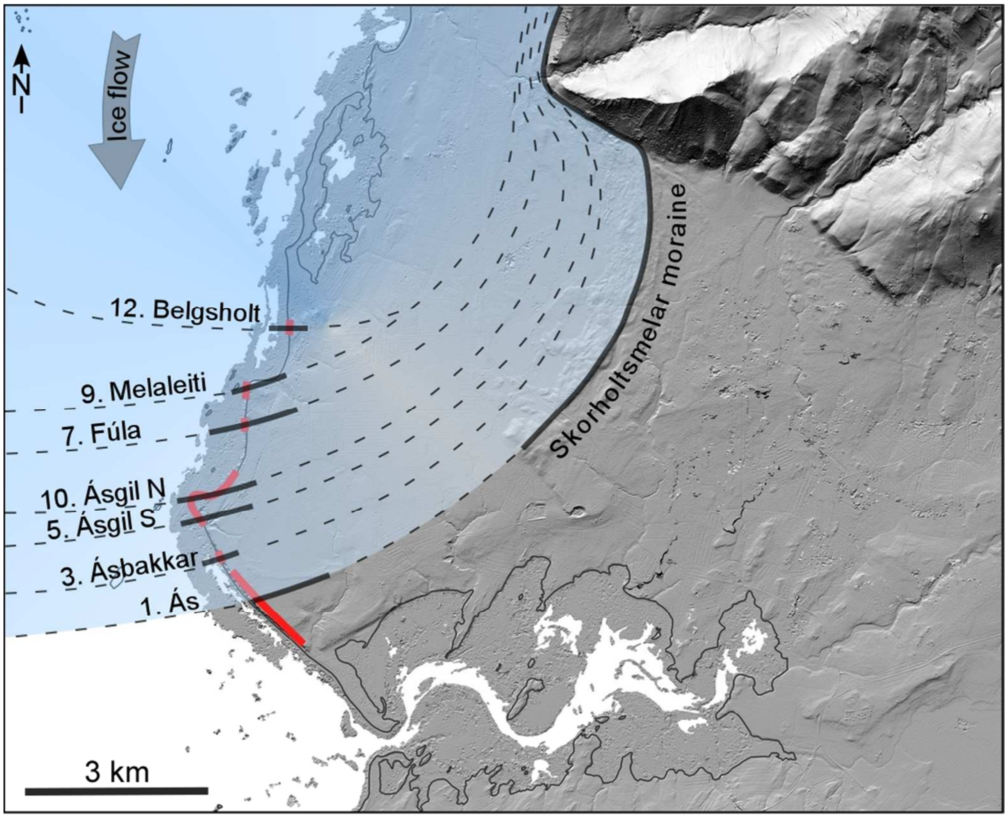

94x76mm (300 x 300 DPI)